A Stronger Gordon Conjecture and an Analysis of Free Bicuspid Manifolds with Small Cusps

Author: Thomas Crawford

A STRONGER GORDON CONJECTURE AND AN ANALYSIS OF FREE BICUSPID MANIFOLDS WITH SMALL CUSPS

Thomas Crawford

A dissertation

submitted to the Faculty of

the department of Mathematics

in partial fulfillment

of the requirements for the degree of

Doctor of Philosophy

Boston College
Morrissey College of Arts and Sciences
Graduate School
May 2018

A Stronger Gordon Conjecture and an Analysis of Free Bicuspid Manifolds with Small Cusps

Thomas Crawford

Advisor: Robert Meyerhoff

Thurston showed that for all but a finite number of Dehn Surgeries on a cusped hyperbolic 3-manifold, the resulting manifold admits a hyperbolic structure. Global bounds on this number have been set, and gradually improved upon, by a number of Mathematicians until Lackenby and Meyerhoff proved the sharp bound of 10, which is realized by the figure-eight knot exterior. We improve this result by proving a stronger version of Gordon's conjecture: that excluding the figure-eight knot exterior, cusped hyperbolic 3-manifolds have at most 8 non-hyperbolic Dehn Surgeries.

To do so we make use of the work of Gabai et. al. from a forthcoming paper which parameterizes measurements of the cusp, then uses a rigorous computer aided search of the space to classify all hyperbolic 3-manifolds up to a specified cusp size. Their approach hinges on the discreteness of manifold points in the parameter space, an assumption which cannot be made if the manifolds have infinite volume. In this paper we also show that infinite-volume manifolds, which must be Free Bicuspid, can have cusp volume as low as 3.159. As such, these manifolds are a concern for any future expansion of the approach of Gabai et. al.

Contents

1 Introduction

A common approach in the study of hyperbolic 3-manifolds is to take an ideal triangulation, together with face pairings, and then ask questions about the manifold itself. The popular program SnapPy [CDGW] is a practical tool to work with manifolds by doing exactly this. A user specifies a manifold in one of a number of ways, then SnapPy calculates a triangulation and returns information about the manifold, such as its volume, fundamental group, and cusp shape. Throughout this paper we work in the opposite direction: we specify what we want or expect the cusp to look like, and then ask questions about the manifold as a whole. For starters we must ask if our specified cusp is compatible with a manifold in the first place.

In a forthcoming paper, Gabai et. al. [GHM$^+$] investigate cusped orientable hyperbolic 3-manifolds of small cusp size by parameterizing the actions of isometry elements. They define six (real) parameters governing the actions of three of these isometries, which if certain criteria are met, represent the generators of the fundamental group of a hyperbolic 3-manifold. The authors limit themselves to a bounded region of this parameter space, only looking at points yielding cusp area less than 5.24. Then then conduct a rigorous computer assisted search of this region and conclude that any cusped hyperbolic 3-manifold with area less than 5.24 must arise from Dehn Surgery on one of 22 specified two and three cusped manifolds.

In this paper we will exclusively work with orientable hyperbolic 3-manifolds.

1.1 Gordon Conjecture

In Section 3 we use the new results from Gabai et. al. to prove a stronger version of Cameron Gordon's [Gor98] conjecture on the number of exceptional (non-hyperbolic) Dehn Surgeries of an orientable cusped hyperbolic 3-manifold. Whereas Lackenby and Meyerhoff [LM08] proved that the number of exceptional surgeries is at most 10 for an orientable hyperbolic 3-manifold (a bound realized by the figure-8 knot

exterior), we further prove that this number is at most 8 for all such manifolds except the figure-8 knot exterior.

1.2 Free Bicuspid

As a result of Mostow [Mos68], Marden [Mar74], and Prasad [Pra73], points corresponding to finite-volume hyperbolic 3-manifolds are isolated in the parameter space of Gabai et. al. One manifestation of this can be seen through the restrictions identity words of the fundamental group place on which particular values of parameters can yield a discrete group. The isolation of these parameter points (stemming from the identity words) is crucial in the approach of Gabai et. al.

In Section 5 we investigate what circumstances cause this isolation to be lost. In other words, we wish to find instances of hyperbolic 3-manifolds with few or no identity words in their fundamental groups (free bicuspid manifolds), yet with parameter values close to those studied by Gabai et. al.

Ian Agol [Ago10] proved that any free bicuspid manifold must have cusp volume at least π. He also constructed an example of a free bicuspid manifold with volume $2\sqrt{3} \approx 3.464$ and found in the SnapPy census a free bicuspid manifold with volume ≈ 3.238. We present constructed examples of free bicuspid manifolds with cusp volumes currently as low as 3.158, as well as a technique that we believe can yield examples with even lower volume.

Agol also proved that any infinite-volume cusped hyperbolic 3-manifold must be free bicuspid. In light of this we are searching for the infinite-volume manifold with the smallest possible cusp.

2 Background

2.1 Isom$^+(\mathbb{H}^3)$ and PSL$(2,\mathbb{C})$

Hyperbolic 3-manifolds cannot be embedded in Euclidean 3-space. To study them we must therefore work within the context of some model. While there are several models of hyperbolic 3-space ($\mathbb{H}^3$), for our purposes the Upper Half Space Model makes many calculations easier. We define $\mathbb{H}^3 = \{x, y, z | z > 0\}$ with the metric $ds^2 = \frac{dx^2+dy^2+dz^2}{z^2}$. The boundary of this space is $\hat{\mathbb{C}} = \mathbb{C} \cup \{\infty\}$ which we can view as a sphere with 0 and ∞ as opposite poles.

In this model geodesics, the continuation of the shortest path between two points, are semi-circular arcs in $\{(x, y, z) | z > 0\}$ that meet $\mathbb{C}$ at right angles, as well as vertical rays which also must meet $\mathbb{C}$ at right angles. Similarly geodesic planes are hemispheres meeting $\mathbb{C}$ at right angles or euclidean planes perpendicular to $\mathbb{C}$.

We are particularly interested in orientation preserving isometries of $\mathbb{H}^3$ which we denote Isom$^+(\mathbb{H}^3)$. These isometries are maps from $\mathbb{H}^3$ to itself which preserve distances and orientation. To work with these maps directly, we look at their representation in $PSL(2,\mathbb{C})$, the orientation preserving 2x2 matrices with coefficients in $\mathbb{C}$ and determinant 1. We associate an element $\gamma = \begin{pmatrix} a & b \\ c & d \end{pmatrix}$ of $PSL(2,\mathbb{C})$, with the isometry $\gamma : z \mapsto \frac{az+b}{cz+d}$. In this paper we use these two interchangeably (hence the abuse of notation with γ), and usually use γ when referring to either the isometry or the matrix.

Strictly speaking, these isometries act on the boundary $\hat{\mathbb{C}}$ of our model, however they can be extended to $\mathbb{H}^3$, so we also view them as acting on $\mathbb{H}^3$.

2.2 Classification of Isometries

We classify the different types of orientation preserving isometries of $\mathbb{H}^3$ as either Parabolic, Elliptic, or Loxodromic. To distinguish between these we pay attention

to the fixed points of a given isometry. When viewing an isometry in the context of its representation in $PSL(2,\mathbb{C})$, we can use the trace $Tr(T) = a + d$ to make the classification.

An isometry is *parabolic* if $Tr(T)^2 = 4$. These isometries have a single fixed point in the bounding plane $\hat{\mathbb{C}}$. We often look at the parabolics fixing the point at infinity, which are of the form $T = \begin{pmatrix} 1 & m \\ 0 & 1 \end{pmatrix}$, so $T : z \mapsto z + m$. It should be noted that any two parabolics with the same fixed point commute.

Isometries are classified as *elliptic* if $Tr(T)$ is real and $Tr(T)^2 < 4$. These elliptics fix two points on $\hat{\mathbb{C}}$ as well as the geodesic joining them, and induce a rotation around this geodesic. For our purposes we usually require that a fundamental group to be discrete and torsion free, meaning that it cannot contain an elliptic isometry since any discrete subgroup generated by an elliptic element must have finite order.

In the final case we say an isometry is *loxodromic*. Here $Tr(T) \in \mathbb{C} \setminus [-2, 2]$. These loxodromic transformations fix two points on $\hat{\mathbb{C}}$, but no points in the interior of $\mathbb{H}^3$. Loxodromic isometries can be thought of as a translation in the direction of a geodesic, together with a rotational around the geodesic. Some definitions distinguish between loxodromic isometries which have a rotational element from those which do not, calling the latter *hyperbolic* isometries, however we will lump the two together and call both cases loxodromic.

2.3 Kleinian Groups and Fundamental Domains

A group Γ is a *Kleinian Group* if it is a discrete subgroup of $PSL(2,\mathbb{C})$. Often we require Γ to be torsion-free, and take Γ to be isomorphic to the fundamental group π_1 of a hyperbolic 3-manifold M, in this case $M = \mathbb{H}^3/\Gamma$. We now have three isomorphic groups: subgroup of $PSL(2,\mathbb{C})$, a group of isometries in $Isom^+(\mathbb{H}^3)$, and a fundamental group $\pi_1(M)$. Through an abuse of notation, we name all three groups Γ.

Let Γ be a torsion-free Kleinian group. A *fundamental domain* for Γ is a region $R \subset \mathbb{H}^3$ such that

- $R \cap \gamma R = \emptyset$ for any $\gamma \in \Gamma \setminus \{1\}$
- $\bigcup_{g \in \Gamma} \overline{gR} = \mathbb{H}^3$

There are many ways to construct fundamental domains, and certain approaches can generate domains with additional nice properties such as convexity and local finiteness. We define one of these constructions, the Dirichlet Domain, as follows. For some point $z_0 \in \mathbb{H}^3$, R_{z_0} is the set of points closer to z_0 than to any $\gamma(z_0)$ for $\gamma \in \Gamma$. That is

$$R_{z_0} = \bigcap_{\gamma \in \Gamma \setminus \{1\}} \{z \in \mathbb{H}^3 | d(z, z_0) < d(z, \gamma(z_0))\}$$

.

This gives us a concrete (in the relative sense) model of the hyperbolic 3-manifold $M = \mathbb{H}^3/\Gamma$. Since Γ is discrete, this region R_{z_0} tiles the universal cover $\mathbb{H}^3$ through the action of Γ. In the case that Γ is geometrically finite, z_0 can be chosen so that R_{z_0} has finitely many faces. One common way to keep track of the manifold itself is to use the polyhedron constructed in this way, together with a set of face pairings (information about which face gets mapped to what other face under an element of Γ). The aforementioned program SnapPy does precisely this.

Note that the shape of R_{z_0} is heavily dependent on the choice of z_0. In fact it often is useful to take z_0 to be a point on the boundary of $\mathbb{H}^3$. With slight adjustments to the definition, to account for what is meant by the distance to a point on the bounding plane, we can generate another type of fundamental region known as a *Ford Domain*. For each $\gamma = \begin{pmatrix} a & b \\ c & d \end{pmatrix} \in \Gamma$ with $c \neq 0$, the isometric sphere I_γ is the plane defined by the circle with center $-c/d$ and radius $1/|c|$. The Ford Domain is the intersection of the half spaces defined by I_γ which include the point z_0.

2.4 Cusps

A manifold M is hyperbolic if it admits a complete hyperbolic metric. By the Margulis Lemma [Thu97], such a manifold M can be decomposed into thick and thin components based on the injectivity radius at a given point. The unbounded portions of the thin components are *cusps*, which are regions that are isomorphic to $T^2 \times [1, \infty)$.

Let Γ be a torsion-free Kleinian group. If Γ has a parabolic subgroup then M/Γ is non-compact and contains a cusp. Take a maximal parabolic subgroup $P < \Gamma$. Recall that parabolic elements that fix the same point commute, so if P has two generators $P = \langle m, n \rangle \cong \mathbb{Z}^2$. It is possible for P to have a single generator ($P \cong \mathbb{Z}$), however in this case the cusp has infinite volume. When a particular point z_0 in $\hat{\mathbb{C}}$ is fixed by P we say M has a cusp at z_0.

If we take a neighborhood of a cusp, expand it until it forms a point of self tangency, then lift it to the the universal cover $\mathbb{H}^3$, we generate what is called a *maximal cusp diagram*, which is typically viewed 'downward' from the point at ∞. The various lifts of the cusp neighborhood, each of which is isometric to $\{x, y, z | z > 1\}$, are known as *horoballs* (or simply *balls*).

This ball $\{x, y, z | z > 1\}$ itself we call B_∞ since parabolics fixing ∞ also fix B_∞. The other horoballs are realized in our model of $\mathbb{H}^3$ as euclidean spheres tangent to $\mathbb{C}$ in a single point, which we call the basepoint. We often reference a horoball by its basepoints. For example, we typically rotate the maximal cusp diagram so that a ball B_∞ is at ∞ and a ball B_0 has basepoint at 0. We also typically normalize so that B_∞ meets B_0 at the point $(0, 0, 1)$.

Since much of this paper is concerned with how these horoballs sit relative to each other, known as horoball packing, we make a few observations here:

- No two horoballs can intersect on their interior, so since the ball B_0 has radius $1/2$, no horoballs other than B_∞ can have radius $r > 1/2$. We call any horoball with radius $1/2$ a full-sized horoball.
- If $P = \langle m, n \rangle$ is the parabolic subgroup that fixes ∞, then the isometries of P map B_0 to other full-sized horoballs, arranged in a lattice generated by the parallelogram that is the fundamental region of P.
- According to Adams [Ada87], there must be a full-sized horoball not of the form $t(B_0)$ where $t \in P$. This "Adams horoball" can be found by taking the inverse of the isometry that takes B_∞ to B_0. In the maximal cusp diagram we also see other full-sized horoballs that form the orbit of this ball B_A under P.

The area of a cusp normalized to B_∞ is the area of the parallelogram spanned by the parabolics fixing ∞, while the cusp volume is the volume of the region above this parallelogram at height 1. A straightforward calculation shows that for cusp C, $\text{vol}(C) = \text{area}(C)/2$.

2.5 Dehn Surgery and Exceptional Slopes

Isotopy classes of simple closed curves on a torus T^2 can be represented by the *slope* of the curve. We write these slopes as reduced fractions $p/q \in \mathbb{Q} \cup \infty$. Given a hyperbolic 3-manifold M with cusp C, *Dehn Surgery* is the process of replacing the neighborhood of a cusp $N(C)$ (which has boundary T^2) with a solid torus $S^1 \times D^2$. This can be done in a number of ways, so we keep track of which slope on $\partial N(C)$ bounds a disk in $S^1 \times D^2$. We call such a Dehn Surgery $s = p/q$ surgery or (p, q) surgery, where p denotes the number of meridian passes while q denotes the number of longitudinal passes. We denote the resulting manifold $M(p, q)$ or $M(s)$. For a particular cusp neighborhood of a manifold M, the length of a surgery slope (p, q) is determined by the translation lengths of the parabolics fixing ∞. In general, manifolds with larger cusps (equivalently in volume and in area), will have fewer short surgery slopes than

manifolds with smaller cusps.

Dehn Surgeries are of particular significance thanks to Lickorish and Wallace's [Lic62] theorem stating that any closed orientable 3-manifold can be obtained by Dehn surgery on a link in S^3.

Thurston's hyperbolic Dehn Surgery theorem [Thu97] asserts that for a cusped hyperbolic 3-manifold M, for all but finitely many Dehn Surgeries (p, q), $M(p, q)$ admits a hyperbolic structure. Any surgery (p, q) for which this is not the case is known as exceptional. The question of exactly how many exceptional slopes are possible has been the subject of much study. After studying many manifolds using SnapPy, and observing that the figure-eight knot exterior has 10 exceptional surgery slopes, Cameron Gordon conjectured that no manifold can have more than 10. This has become known as the Gordon Conjecture. However he further conjectured (Conjecture 3.3 in [Gor98]) that other than in the case of the figure-eight knot exterior, the number of exceptional surgery slopes is at most 8. By applying results from [GHM$^+$] and continuing the work of those discussed below, we prove this "Strong Gordon Conjecture."

In the introduction of their paper, Lackenby and Meyerhoff [LM08], discusses several parallel approaches to the question various researchers have taken. Many of these take made use of topological arguments: analyzing what types of surfaces can be embedded in the manifold, looking at foliations or laminations, or taking a combinatorial approach to the crossing number of essential surgery slopes.

We however take a geometric approach, continuing in the tradition of Gromov and Thurston [GT87] whose 2π-*Theorem* asserted that any essential surgery must be along a slope of length less than 2π as measured on the maximal cusp neighborhood. This 2π-Theorem gave an upper bound of 48 essential surgeries, which was later improved to 24 by Bleiler and Hodgson [BH96], then to 14 by Cao and Meyerhoff [CM01]. Independently Lackenby [Lac00] and Agol [Ago00] improved the theorem to the *6-Theorem* which further improved the upper bound on essenential surgeries to 12.

Through the use of Mom-technology and observations about the length spectrum of isometries in a cusped manifold, Lackenby and Meyerhoff [LM08] managed to reduce this bound to 10, thus proving the original Gordon Conjecture.

2.6 SnapPea, SnapPy, Regina, and others

SnapPea, and its python implementation SnapPy [CDGW], are tools to study the hyperbolic structure of 3-manifolds. A user can specify a manifold by drawing a link (to look at its exterior), by specifying exact tetrahedra and face pairings, or by choosing from a census of pre-calculated manifolds ordered by the minimum number of tetrahedra required. The program then does all the heavy lifting in regards to keeping track of tetrahedron size, shape, face pairings, and Dehn Surgeries. SnapPea can then return a host of information about the Manifold, including the specifics of the cusp shape and size, and can even draw a maximal cusp diagram.

When we use SnapPy in the context of the Gordon Conjecture we are particularly interested in whether or not a Dehn-Filled cusped manifold admits a hyperbolic structure. SnapPea primarily uses Newton's method to solve gluing equations as floatingpoint parameters. Since these are inexact, SnapPea cannot definitively say if a solution it finds indicates the presence of hyperbolic manifold. Recent updates of SnapPy have remedied this by implementing a .verify() method based off HIKMOT [HIK$^+$99] and SNAP [Goo]. The solutions to the equations SnapPy works with are typically algebraic numbers, so this verify method uses an LLL algorithm to find polynomials for which these parameters are zeros. Such a solution can be used to guarantee that a particular solution is a hyperbolic 3-manifold. SnapPy also recently developed support for rigorous cusp translation calculations, which we make use of.

We occasionally also wish to show that a particular manifold $M(p, q)$ is not hyperbolic. When SnapPy attempts to analyze such a manifold it either fails to construct a triangulation or constructs a triangulation with degenerate tetrahedra. Unfortunately SnapPy's construction can also fail for a number of reasons so this does not neces-

sarily indicate that a manifold is not hyperbolic. As a result of Perelman's solution to the Geometrization Conjecture [Per02], a manifold is either hyperbolic, reducible (contains an essential 2-sphere), toroidal (contains an essential torus), or Seifert Fibred (is foliated by circles). Therefore if we can find such a structure, the manifold cannot be hyperbolic. To do this we use a program by Haraway [Har] running in Regina [BBP+17], a software package that rigorously identifies normal surfaces.

Haraway's script checks for surfaces known as *faults* which include:

- Non-orientable surfaces with $\chi \geq 0$
- Spheres S^2 which do not cut off a 3-ball
- Disks which do not cut off a 3-ball
- Tori which are not boundary compressible and do not cut off $T^2 \times I$
- Annuli which cut off neither a 3-ball nor $D^2 \times S^1$

Failing to find such a fault, the script checks the fundamental group for evidence that it is Seifert Fibred, such as looking for an infinite cyclic monodromy group. While this procedure is not guaranteed to show that a non-hyperbolic triangulation is in fact not hyperbolic, it has succeeded every time we have used it.

2.7 SnapPy Census

Using their program SnapPea, Hodgson and Weeks constructed censuses for manifolds of various types including cusped orientable manifolds, closed orientable manifolds, link exteriors, and non-orientable manifolds. We are particularly interested in the census of cusped orientable manifolds, which includes the 61,911 manifolds that can be constructed with up to 9 ideal tetrahedra. Hodgson and Weeks also gave a name to each of these manifolds such as m004 and s776, where the first letter indicates the number of tetrahedra with which it was constructed. Manifolds beginning with m can be constructed with 5 or fewer tetrahedra, manifolds with s use 6 tetrahedra, continuing with v for 7, t for 8, and o for 9.

Occasionally a statement we make will apply to a collection of manifolds with names all beginning with the same number. While this is usually a coincidence, the manifolds beginning with m and s are in many senses simpler than those beginning with v, t, or o, so there is occasionally some insight to be gained by paying attention to the names of the manifolds.

2.8 Hyperbolike vs Hyperbolic

Traditionally a closed orientable 3-manifold that was atoroidal, irreducible, and not a Seifert Fibred space was said to be *hyperbolike*. These manifolds were conjectured to be in fact hyperbolic manifolds, however this was not proven until Perelman proved the Geometrization Conjecture 2003. This conjecture of Thurston states that any 3-manifold can be canonically broken up into pieces, each of which have one of eight geometries. As a consequence of this, hyperbolic 3-manifolds must be toroidal, irreducible, Seifert Fibred, or hyperbolic. In light of this, papers published after the early 2000s make no distinction between hyperbolike and hyperbolic.

2.9 The Parameter Space of Gabai et. al.

By parameterizing the isometries $\langle m, n, g\rangle$, and analyzing the 6-real-dimensional parameter space, Gabai et. al. [GHM$^+$] prove the following:

Theorem 2.1. *(Gabai et. al.) Let M be a cusped orientable finite-volume hyperbolic 3-manifold and C be the maximal horoball neighborhood of a cusp. If $area(C) \leq 5.24$ then M is a Dehn Surgery of one of the following 22 manifolds.*

m125	m129	m203	m292	m295				
s443	s596	s647	s774	**s776**	s780	s782	s785	
v2124	v2355	v2533	v2644	v2731	v3108	v3127	v3211	v3376

It should be noted that all are two-cusped manifolds save $s776$, the so-called magic manifold, which has three cusps.

The proof of this involves searching the parameter space for points whose representative isometries form a torsion-free Kleinian group, and therefore correspond to an orientable hyperbolic 3-manifold. The authors break the parameter space into regions or chunks, declaring many to not contain any manifold points for one reason or another, most often because the parameter values in the region correspond to isometries that form a non-discrete group. After this process is repeated a number of times for smaller and smaller chunks, they are left with 2-dimensional varieties in the parameter space which contain many of the points they are looking for. These varieties and the manifold points on them arise as Dehn Surgeries on one of the above manifolds, known as 'variety manifolds' for this reason.

Using the Gromov norm, Thurston [Thu97] proved that under Dehn Surgery the volume of a manifold decreases. While it is not necessarily true that the volume of one cusp of a multi-cusped manifold decreases under Dehn Surgery on another cusp, we usually observe this to be the case. It can also be observed that for multi-cusped manifolds, higher order surgeries (surgery slopes with greater length) on one cusp result in volumes and cusp volumes (of the other cusp) that approach the original manifold.

The first 7 manifolds in the table of Theorem 2.1 have a cusp with area ≤ 5.24 (volume ≤ 2.62). As such, they correspond to a variety in the parameter space with a countably infinite number of manifold points. That is for each of the first 7 manifolds in the table, as well as 20 additional two-ocusped manifolds formed by Dehn Surgery on s776, countably many manifolds with cusp area ≤ 5.24 can be derived from Dehn Surgery. For the remaining manifolds in the table, only finitely many Dehn Surgeries correspond to manifold points with cusp area ≤ 5.24.

Figure 2.1 depicts a number of surgeries on five manifolds (chosen from the list of 22 to be intentionally spaced out) and plots the isometries m and n vs the cusp volume. Being a 3-dimensional plot, this is obviously only a slice of the 6-dimensional parameter space, but it gives us insights into how the varieties intersect the space.

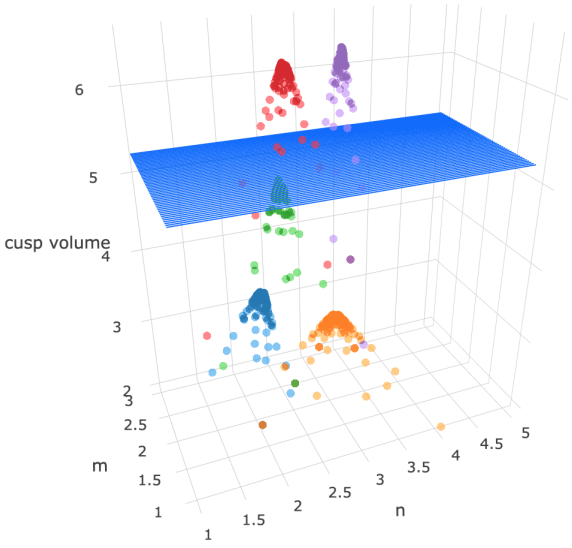

Figure 2.1:

Blue: m135,
Orange: m129,
Green: s596,
Red: v3211,
Purple: v3376

Specifically we can see that some variety two-cusped manifolds have a cusp area ≤ 5.24 and that most surgeries result in a manifold point within the ≤ 5.24 region. We also see that other variety manifolds themselves lie outside this region and only finitely many surgeries yield manifolds with ≤ 5.24.

Though the manifolds in Theorem 2.1 correspond to accumulation points in the parameter space, the points for all other manifolds are isolated. In other words since these are finite manifolds any deformation or continuous change in parameter values cannot result in another hyperbolic manifold. As we show in Sections 5 and 6, this is no longer true of manifolds with cusp area as small as 6.32. One motivation for this project is to investigate what occurs in this transition. We wish to know for what region in the parameter space are points isolated, and what the boundary of this region looks like.

2.10 Necklaces and Dehn Surgery

In the search of their parameter space, Gabai et. al. discovered varieties, or families of manifolds with similar parameter values having in common the fact that they were Dehn Surgeries of one of the variety manifolds in Table 3.1.

For now we define necklaces to be sequences of tangent horoballs. Often we look at necklaces which include B_∞ which are seen as chains, or sequences of tangent horoballs, connecting full-sized horoballs. Dehn surgery on one cusp of a multi-cusped manifold also preserves necklaces in the other cusp, up to some resizing. Take for example the manifold $v3376$. Figure 2.2 illustrates a sequence of surgeries which preserve the blue and yellow necklaces. There is also a correlation between the order and the length of the chain marked in green. Higher order surgeries limit towards the unfilled case of $v3376$, where the green chain does not connect.

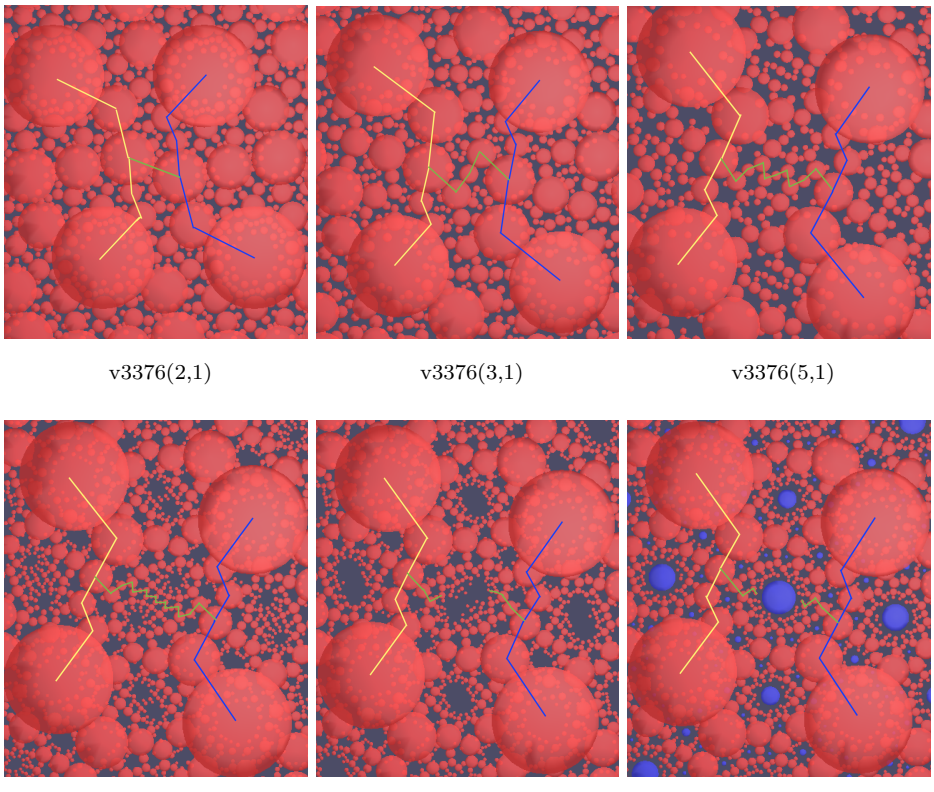

Figure 2.2: Drawn with SnapPy. Various surgeries on v3376, with two necklaces represented by the yellow and blue lines. In green are chains of horoballs connecting the two necklaces. In the v3376(12,1) case the green chain does not break off, rather the resolution of SnapPy will not show horoballs below a certain size.

We will later work with free bicuspid manifolds; manifolds whose cusps do not have any such necklaces.

3 The Strong Gordon Conjecture

In this section we prove the Strong Gordon Conjecture:

Theorem 3.1. *Let M be a cusped orientable finite-volume hyperbolic 3-manifold. If M is not isotopic to the figure-eight knot exterior (m004), then M has at most 8 exceptional Dehn Surgeries.*

To do so we utilize the "6-Theorem" of Agol and Lackenby:

Theorem 3.2. *(Agol, Lackenby): When the length of each surgery slope $s_1, ..., s_n$ is greater than 6, $M(s_1, \ldots, s_n)$ is hyperbolic.*

3.1 Proof of the Strong Gordon Conjecture

Recall from Theorem 2.1 of Gabai et. al. that any cusped 3-manifold with cusp area ≤ 5.24 comes from Dehn Surgery on one of the following 22 manifolds:

m125	m129	m203	m292	m295				
s443	s596	s647	s774	s776	s780	s782	s785	
v2124	v2355	v2533	v2644	v2731	v3108	v3127	v3211	v3376

Table 3.1

This allows us to split the proof of the Strong Gordon Conjecture into two cases: one-cusped manifolds with cusp area ≥ 5.24, and manifolds that arise from Dehn Surgery on one of the above 2 and 3-cusped manifolds. We address the former with the following theorem, and the latter on a case-by-case basis. It should be noted that Agol [Ago10] proved an equivalent version of this theorem. We include this version because the proof is more direct and because this approach gives a stronger, more adaptable result if generalized to address the ≤ 7 case.

Theorem 3.3. *Let M be a cusped orientable finite-volume hyperbolic 3-manifold, and for one of the cusps let the area of the maximal cusp torus $A > 36/7 \approx 5.14$. At most 8 Dehn Surgeries on this cusp can be exceptional.*

Proof. We consider possible pairs of parabolic isometries σ, τ fixing ∞ of the filled manifold $M(p, q)$, and show the lattice formed by these isometries can feature at most 8 primitive lattice points. Here we define lattice point $p\sigma + q\tau$ to be primitive if p and q are coprime. We parameterize σ, τ with real parameters a, b, and m such that $\sigma : 0 \mapsto m$ and $\tau :\mapsto a + bi$ with

- $|a + bi| \geq m \geq 1$
- $0 \leq a < m/2$
- $b > 0$
- $mb > A = 36/7$

Let N_q be the number of primitive lattice points of the form $p\sigma + q\tau$ with $|p\sigma + q\tau| \leq 6$. That is, let N_0 be the number of points formed with no instances of τ, N_1 the number of points with one instance of τ, etc. Observe that $N_0 = 1$ and since $|a + bi| \geq m$, $N_p = 0$ for $p \geq 3$.

On a circle of radius 6, the length of a chord a distance b from the origin is $2\sqrt{6^2 - b^2}$. Primitive points contributing to N_1 are a distance m apart, Therefore

$$N_1 \leq \lfloor \frac{2\sqrt{6^2 - b^2}}{m} + 1 \rfloor = \lfloor \frac{2\sqrt{36 - (A/m)^2}}{m} + 1 \rfloor \leq \lfloor \frac{36}{A} + 1 \rfloor \leq 7 \tag{1}$$

Similarly since primitive points with two instances of τ (points that contribute to N_2) are spaced $2m$ apart we have:

$$N_2 \leq \lfloor \frac{2\sqrt{6^2 - (2b)^2}}{2m} + 1 \rfloor = \lfloor \frac{\sqrt{36 - (2A/m)^2}}{m} + 1 \rfloor \leq \lfloor \frac{9}{A} + 1 \rfloor \leq 2 \tag{2}$$

Our next two claims cannot be proven with this chord length argument alone. Instead we take into account the 'shift' values of a. Since $0 \leq a < m/2$, the closest primitive point to the origin featuring 2τ is $2\tau - \sigma$ while the second is $2\tau + \sigma$. Similarly the sixth and seventh closest points with a single τ are $\tau - 3\sigma$ and $\tau + 3\sigma$ respectively. See Figure 3.1. We wish to show that for $A > 36/7$, for combination of values of a

and m we cannot have both two primitive points at N_2 and six primitive points at N_1.

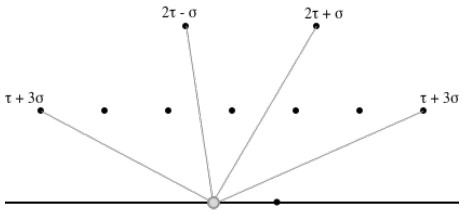

Figure 3.1: The 10 relevant lattice points for the following cases

If $N_2 = 2$, then

$$|2(a+bi)+m| < 6 \tag{3}$$

$$\Rightarrow \quad (2a+m)^2 + (2A/m)^2 \leq 36 \tag{4}$$

$$\Rightarrow \quad a \leq -\frac{m}{2} + \frac{\sqrt{9m^2 - A^2}}{m} \tag{5}$$

$$\Rightarrow \quad a < 3m - \frac{\sqrt{36m^2 - A^2}}{m} \qquad (when\ A > \frac{36}{7}) \tag{6}$$

$$\Rightarrow \quad (3m-a)^2 + (A/m)^2 > 36 \tag{7}$$

$$\Rightarrow \quad |(a+bi) - 3m| > 6 \tag{8}$$

$$\Rightarrow \quad N_1 < 6 \tag{9}$$

To shed light on these unintuitive equations, Figure 3.2 plots m vs. a for various values of A, and the regions in which these combinations of a and m satisfy each

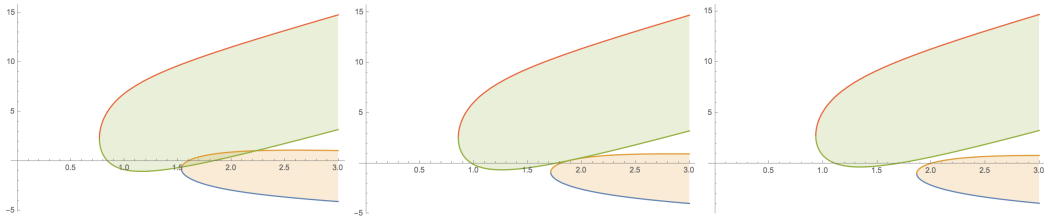

A=4.6 A=5.14 A=5.6

Figure 3.2: With m on the x-axis and a on the y-axis, the green region represents values in which $N_1 = 6$, while the orange region represents values in which $N_2 = 2$. We can see that 'overlap' of the regions does not occur when $A > 36/7$.

By a similar argument, if $N_2 = 1 \Rightarrow N_1 < 7$. Therefore $\sum_p N_p \leq 8$, so cusps with area $A > 36/7$ have at most 8 slopes with length ≤ 6. By the 6-Theorem, these are the only potentially exceptional slopes.

□

This bound of $A = 36/7$ realizes 9 exceptional slopes when $a = \pm 1/5$:

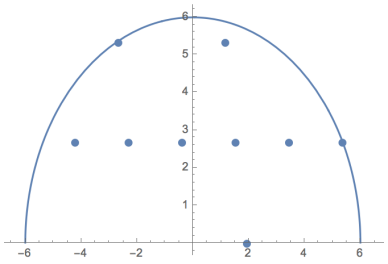

Figure 3.3: With A= 36/7, the lattice formed by m= $\frac{6\sqrt{5}}{7}$, and $n = -\frac{6}{7\sqrt{5}} + \frac{42i}{\sqrt{5}}$ realizes 9 slopes with length ≤ 6.

It now suffices to show that for any manifold (other than m004, the figure-eight knot exterior) resulting from Dehn Surgery on one of the manifolds in Table 3.1, the maximal number of exceptional Dehn Surgeries is 8. Thankfully this already has been proven for many of these manifolds. Martelli and Petronio [MP02] completely classified the Dehn Surgeries of $s776$, also known as the 'magic manifold' or the 3-component chain link. While the techniques we use could be applied to a 3-cusped manifold, the complexity of the process would increase greatly. The classification of $s776$ brings with it the classification of any two-cusped manifold resulting from Dehn Surgery on it. This includes $m125, m129, m203, m292, m295$, and $s443$.

In their proof of the (regular) Gordon Conjecture, Lackenby and Meyerhoff [LM08], classifed the Dehn Surgeries on Mom-3 manifolds, which include $s496$, $s647$, $s774$, $s780$, and $s785$. Other than two appearances of $m004$ ($s647(-1, 2)$, and $s780(0, 1)$), they found no surgeries that resulted in a manifold with more than 8 exceptional surgeries.

We are left with the following two-cusped manifolds to analyze:

s782	v2124	v2355	v2533	v2644
v2731	v3108	v3127	v3211	v3376

Table 3.2

There are a countably infinite number of one-cusped manifolds resulting from surgery on these manifolds. To narrow this down to a finite number of cases, we apply the following corollary of Theorem 3.3.

Corollary 1. *For s with length$(s) > 6$, if one cusp of a two cusp manifold M has area $\geq 36/7 \approx 5.1428$, then the manifold resulting from surgery on the other cusp along s ($M(-, s)$) has at most 8 exceptional surgeries.*

Proof. Since the first cusp of M has area $\geq 36/7 \approx 5.1428$, there are at most 8 surgeries t of the first cusp with length < 6. By the 6-theorem if length$(t) > 6$ and length $(s) > 6$ then $M(t, s)$ is hyperbolic. Therefore the only potentially exceptional surgery slopes of $M(-, s)$ are the 8 for which t has length < 6. □

Since the cusps of the manifolds of Table 3.2 all have area ≥ 5.143, any possible counter-example to the Strong Gordon Conjecture must be $M(s, -)$ or $M(-, s)$ for M in Table 3.2 and *length*$(s) \leq 6$. There are 106 such manifolds. Of these 106, 69 are not hyperbolic. We prove this claim with a straightforward application of Haraway's rigorous Regina script [Har], which finds faults or barriers that prevent a manifold from being hyperbolic (see Section 2.6). The results of this script, including what fault was discovered, can be found in Appendix A. We include a portion of one of these tables here:

s782, cusp 1	
Surgery	Fault
(1,0)	K^2 (non-orientable)
(0,1)	M^2 (non-orientable)
(1,1)	T^2
(-1,1)	π_1 free
(-2,1)	T^2

SnapPy's .identify() method can be used to rigorously identify the cusp census names of the remaining 37 manifolds we constructed by Dehn Surgery on one of the two cusped manifolds in Table 3.2. This reveals a number of duplicates, narrowing the list of 37 down to the following 18:

m004	m011	m015	m019	m022	m023
m034	m070	m081	m120	m137	m139
m221	s096	s119	s313	s348	s572

Table 3.3

All of these 18 manifolds except s348 and s572 can be obtained by Dehn Surgery on one of the manifolds of Table 3.1 that have already been analyzed. For these two manifolds if we calculate the cusp translations using SnapPy, again a rigorous computation, we see that despite having cusp area < 5.14, neither have more than 8 slopes of length ≤ 6. Recall that the $36/7 \approx 5.14$ bound only realizes 9 slopes of length ≤ 6 in the optimum case.

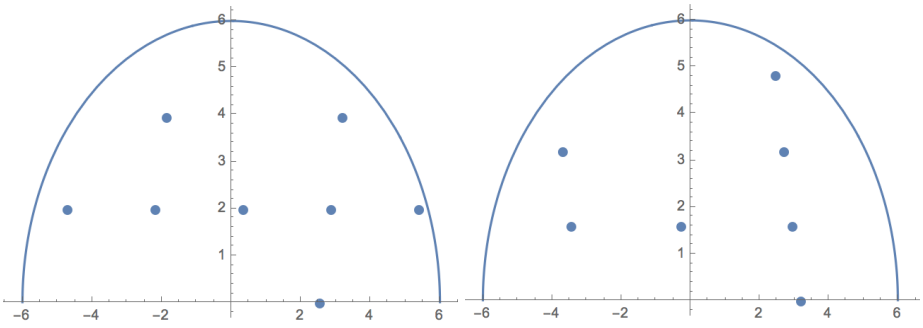

s348 s572

Figure 3.4

Therefore for any Dehn Surgery slope s on a manifold M in Table 3.1, $M(s)$ has at most 8 exceptional surgeries. This completes the proof of Theorem 3.1.

3.2 Further Improvement

Thurston [Thu97] showed that the figure-eight knot exterior has 10 exceptional slopes. With W the Whitehead link exterior $m135$, Hodgson and Weeks [CDGW] showed using SnapPea that $W(5,1)$ has 8 exceptional slopes. Betley, Przytycki and Zukowski [BPZ86] showed that $W(-2,1)$ also has 8 exceptional slopes. In addition to these, 8 have been discovered to have 7 exceptional slopes, and an infinite class of manifolds have 6 exceptional slopes. Gordon states that "In view of this data it is tempting to believe that these eleven manifolds are the only ones with [7 or more exceptional slopes]." Indeed it is tempting to believe this, however proving that $W(-2,1)$ and $W(-5,1)$ are the only manifolds in addition to the figure-eight knot exterior to have 8 exceptional slopes requires a substantial jump beyond what we have proven here.

Expanding our argument to this stronger result would require either an improvement to the 6-theorem or a significant improvement on the 5.24 bound. Relying purely on the 6-theorem would require a categorization of all manifolds with cusp area up to 7.2, a goal which faces several obstacles including, as we see in later sections of this paper, the presence of infinite-volume manifolds with cusp area as low as 6.32.

However not all hope is lost. If the 5.24 area bound of Gabai et. al. can be increased beyond 6, there are various statements that we can make about the shape of the cusp. For example if $A > 6.235$ then $N_1 \leq 5$, which forces the parabolic lattice to be 'boxy' ($|m| \approx |n|$). Lackenby and Meyerhoff use information about $\mathcal{O}(2)$ to improve the 6-Theorem in specific cases, so it is certainly possible that a similar improvement can be developed for a specific statement along the lines of $|m| \approx |n|$).

Regardless it seems implausable that this approach to the Strong Gordon Conjecture can be extended to the ≤ 7 'Stronger Gordon Conjecture' without substantial improvement to the 5.24 area bound of Gabai et. al.

4 Free Bicuspid Definitions and Notation

Let Γ have parabolic subgroup $P = \langle m, n \rangle$. While $\Gamma = P$ is a torsion-free Kleinian group, it is not a particularly interesting Kleinian group, so we typically assume that P has one more generator, g. We are primarily interested in the case where Γ can be expressed with exactly these three generators. As Gabai et. al. showed, this is sufficient for manifolds with small enough cusp. Since m, n commute, we write $\Gamma = \langle m, n, g | mnMN \rangle$ where M and N are the inverses of m and n. We say that Γ is *free bicuspid* if $mnMN$ is the only identity word in Γ. That is, if $\Gamma \cong \langle m, n \rangle * \langle g \rangle$. In the case where Γ has additional generators, Γ is free bicuspid if it has a subgroup with the above property.

We say that any hyperbolic 3-manifold with a free bicuspid fundamental group is a free bicuspid manifold. If a free bicuspid manifold has multiple cusps, we say that each cusp C is free bicuspid if for some parabolic P fixing a lift of C, $\Gamma \cong P * Q$ for some Q. In this section we primarily work with manifolds with a single cusp, however Figure 4.1 depicts a three-cusped manifold with only one free bicuspid cusp.

4.1 Chains and Necklaces

As in [AK12], we define two horoballs as being *tangent* if the point of intersection of their boundaries is a lift of the intersection between B_∞ and $g(B_\infty)$. Let $H = \{tg^{\pm}(B_\infty)|t \in P\}$ be a collection of full-sized horoballs. It is entirely possible for maximal cusp diagrams to feature additional full-sized horoballs. While the boundary of these full-sized horoballs is strictly speaking tangent to the ball at infinity, we make the distinction between these points of tangency and those corresponding to lifts of g and G. We say only the latter that the balls themselves are tangent.

For any given horoball B there is some associated word (element) $\omega \in \Gamma$ for which $\omega(B_\infty) = B$. Let $H = \{tg(B_\infty)|t \in P\} \cup \{tG(B_\infty)|t \in P\}$ be a collection of full-sized horoballs. Since P fixes B_∞, this is the complete list of horoballs tangent to B_∞. Similarly for any horoball B_1 with word ω_1, if B_2 is tangent to B_1, then B_2 can be described by word $\omega_1 tg^{\pm}$.

One useful tool for the study of these words ω and the associated horoballs B is the *g-number* of the word. We define this to be the number of instances of g or G in a simplified word ω. We can think of the maximal cusp diagram as being developed "outward" from B_∞ by repeating this process of considering all the horoballs tangent to it, then the horoballs tangent to those, etc. Any particular horoball B_1 therefore has a *chain*, or sequence of tangent horoballs, leading back to B_∞. By this logic, horoballs with greater g-number are out farther than tangent balls with lesser g-number.

This chain is only unique in the free bicuspid case. We define a *necklace* to be a cycle of tangent horoballs. If a maximal cusp diagram has a necklace then there must be multiple words ω_1 and ω_2 associated to a given horoball, so there must be an additional identity word, $\omega_1^{-1}\omega_2 = 1$, in $\langle m, n, g\rangle$. Therefore $\langle m, n, g\rangle$ is not free bicuspid.

4.2 Prior Examples

As mentioned in Section 1, Ian Agol did a search of the SnapPy census for free bicuspid manifolds with low cusp volume. The best example (smallest cusp volume) he found was a 3-fold cover of v1902 with cusp volume 3.238. Notice in Figure 4.1 the lack of necklaces formed by the red horoballs.

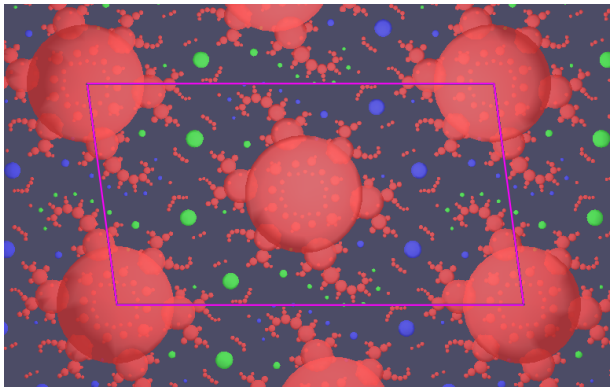

Figure 4.1: One of the 3-fold covers of v1902. The red cusp is free bicuspid and the other two cusps are reduced in size. This manifold has cusp volume 3.238.

Also worth pointing out in this example is the fact that the manifold has finite volume. While all infinite-volume manifolds are free bicuspid, the converse is not necessarily true. However we have only been able to find examples of finite volume manifolds with multiple cusps; the other cusps take up the space in the gaps left by the spiraling arms that form when necklaces are prohibited. We conjecture that any free bicuspid manifold with a single cusp must have infinite volume.

4.3 Formulas

In this paper we will often compare the relative separation of horoballs B_1 and B_2 so we need to have a measure of the distance between them. Since the basepoints z_1 and z_2 of B_1 and B_2 are on the bounding plane, we cannot use the length of the geodesic connection between z_1 and z_2. Instead we say the *ortho-distance* between two horoballs is the length of the line segment of this geodesic which lies outside both horoballs [Mey96]. In practice we use the following formula, derived from the metric

of the upper half space model:

$$d_{hyp}(B_1, B_2) = \ln\left(\frac{|z_1 - z_2|^2}{4r_1 r_2}\right) \tag{10}$$

One can see that if two full-sized horoballs have basepoints a distance a apart, then

$$d_{hyp}(B_1, B_2) = \ln(a^2). \tag{11}$$

Isometries preserve distance, so if the basepoint of a full-sized horoball B_2 is a distance of a from 0, then $g(B_2)$ is a distance of $\ln(a^2)$ from B_∞. A simple calculation shows that $g(B_2)$ must therefore have radius $1/2a^2$.

Given a particular maximal cusp diagram, the ortholength spectrum is the list of possible ortho-distances in ascending order. Since we always have a pair of tangent horoballs, the first ortholength $\mathcal{O}(1) = 0$. In this paper we work with manifolds for which the closest full-sized horoball to B_0 is a euclidean distance of a away.

An elementary calculation shows that given two tangent horoballs with basepoints separated by a euclidean distance d, if one ball has radius r_1, the other has radius

$$r_2 = \frac{d^2}{4r_1}. \tag{12}$$

4.4 Notation

Working in the Euclidean plane $\mathbb{C}$, we will use the shorthand $C(z, r)$ to indicate the circle centered at z with radius r. Similarly we will use $D(z, r)$ to represent the disk with center z and radius r.

For a horoball B with basepoint z_0 and radius r_0, $p(B)$ is the projection down to $\mathbb{C}$ to the circle $C(z_0, r_0)$.

5 A Sufficient Condition for M to be Discrete and Free Bicuspid

Our goal is find an easy to check criterion to determine if a maximal cusp diagram corresponds to a free bicuspid 3-manifold with complete hyperbolic structure. That is, we want to show Γ is discrete and that it is free bicuspid. In this section we take $\Gamma = \langle m, n, g\rangle$ where $\langle m, n\rangle$ are parabolic elements fixing the point at ∞, and g is a loxodromic element.

We will use a to represent the minimum separation of full-sized horoballs. That is, a =min($|z_i|$) for z_i in the collection of basepoints $\{t(0)\} \cup \{t(g(\infty))\}$.

This criterion is as follows:

Theorem 5.1. *Let $\Gamma = \langle m, n, g\rangle$ with $P = \langle m, n\rangle$ fixing ∞, and let $a = min\{|t(0)|, |t(g(0)|\}$ for $t \in P$. If there exist regions Ω_g and Ω_G in $\mathbb{C}$, (let $\Omega = \Omega_g \cup \Omega_G$) such that*

- $\Omega_g \cap \Omega_G = \emptyset$
- $\Omega \cap t(\Omega) = \emptyset$ *for* $t \in \langle m, n\rangle, t \neq 1$
- $g\Big(\bigcup_{t\in P} t(\Omega)) \setminus \Omega_G\Big) \subset \Omega_g$
- $G\Big(\bigcup_{t\in P} t(\Omega)) \setminus \Omega_g\Big) \subset \Omega_G$
- $D(0, \frac{1}{a-1/2}) \subset \Omega_G$
- $D(g(\infty), \frac{1}{a-1/2}) \subset \Omega_g$

Then M/Γ is a free bicuspid hyperbolic 3-manifold.

In Section 6 we define a specific class of manifolds that were constructed in an effort to minimize this separation a while maintaining the conditions of Theorem 5.1. One such construction is depicted in Figure 5.1.

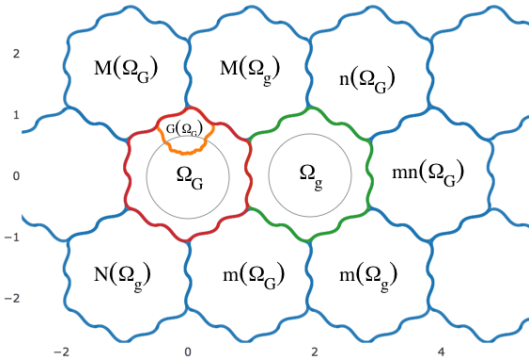

Figure 5.1

5.1 Proving Freeness

In the following Theorem, we view Γ as acting on the bounding plane $\mathbb{C} \cup \{\infty\}$.

Theorem 5.2. *For $\Gamma = \langle m, n, g \rangle$ with $P = \langle m, n \rangle$ fixing ∞, if there exist regions Ω_g and Ω_G in $\mathbb{C}$, (let $\Omega = \Omega_g \cup \Omega_G$), such that*

- $\Omega_g \cap \Omega_G = \emptyset$
- $\Omega \cap t(\Omega) = \emptyset$ *for* $t \in \langle m, n \rangle, t \neq 1$
- $g\Big(\bigcup_{t \in P} t(\Omega)) \setminus \Omega_G\Big) \subset \Omega_g$
- $G\Big(\bigcup_{t \in P} t(\Omega)) \setminus \Omega_g\Big) \subset \Omega_G$

Then Γ is free bicuspid.

Proof. Our proof uses an adaptation of the well-known ping-pong lemma [Har00]. Let $\Omega' = \Big(\bigcup_{t \in P} t(\Omega)) \setminus \Omega\Big)$. Observe that by construction, for any non identity element of $\gamma_1 \in P = \langle m, n \rangle$, we have $\gamma_1(\Omega) \subset \Omega'$. Similarly one can see that for any non identity element $\gamma_2 \in H = \langle g \rangle$, we have $\gamma_2(\Omega') \subset \Omega$. This is clear since any such γ_2 is of the form g^{n_i} or G^{n_j}, and repeated iterations of g map Ω' to Ω_g while repeated iterations of G map Ω' to Ω_G.

We show that any word ω spelled from non-identity letters from P and H cannot be the identity. We have two cases: ω begins and ends with letters from the same subgroup, and w begins and ends with letters from different subgroups.

Suppose $\omega = a_1 b_1 ... b_{j-1} a_j$. Without loss of generality let $a_i \in P$ and $b_i \in H$. Then

$$\begin{aligned} w(\Omega) &= a_1 b_1 ... b_{j-1} a_j(\Omega) \\ &\subset a_1 b_1 ... b_{j-1}(\Omega') \\ &\vdots \\ &\subset a_1 b_1(\Omega') \\ &\subset a_1(\Omega) \\ &\subset \Omega' \end{aligned}$$

So w cannot be the identity. For the second case, if $w = a_1 b_1 ... a_j b_j$, then choose a nontrivial element $a_k \in P$ with $a_k \neq a_1$. Then w cannot be the identity as $a_k w a_k^{-1}$ cannot be the identity.

Therefore $\langle g \rangle$ acts freely on $\langle m, n \rangle$, so we can say $\Gamma = \langle m, n, g | mnMN \rangle$ is a free bicuspid group. □

Corollary 2. *Let $R \subset \Omega_G$ for Γ and Ω_G as above, and let $\omega \in \Gamma$ be a reduced word that ends in any letter but g. Then either $\omega(R) \subset t(\Omega_g)$ or $\omega(R) \subset t(\Omega_G)$ for some $t \in \langle m, n \rangle$.*

Proof. Write $\omega = tg\omega_2$ or $\omega = tG\omega_2$, with $t \in \langle m, n \rangle$. By the same ping-pong action in Theorem 5.2, for any point $z \in \Omega_G$, $\omega(z)$ is in the region $t(\Omega_g)$ or $t(\Omega_G)$, dependent only on the prefix tg or tG. □

5.2 Proving Discreteness

Here we provide a condition under which Γ is guaranteed to be discrete. This proof relies on supporting Propositions in Section 5.3. To motivate these Propositions, we prove Theorem 5.3 here and refer the reader to Section 5.3 for proofs of various claims. Note that since a is the minimum separation of full sized horoballs, $a > 1$.

Theorem 5.3. *Let Γ be defined as above. If there are regions Ω_g and Ω_G in $\mathbb{C}$ as in*

Theorem 5.2, with the additional condition that the disk $D_1 = D(0, \frac{1}{a-1/2}) \subset \Omega_G$ *and* $D_2 = (g(\infty), \frac{1}{a-1/2}) \subset \Omega_g$ *then* M/Γ *is a discrete manifold.*

Proof. By Proposition 5.3 for every horoball B with basepoint in Ω_G, the projection $p(B)$ to the plane $\mathbb{C}$ is covered by $\gamma(D_1)$ for some $\gamma \in \Gamma$ with the word γ ending in G. Since the basepoint of B is in Ω_G, by Corollary 2, $\gamma(D_1) \subset \Omega_G$. Therefore $p(B) \subset \Omega_G$. The identical argument holds for horoballs with basepoints in Ω_g, and an analogous property holds when shifted by a parabolic $t \in \langle m, n \rangle$. Therefore $p(B)$ is contained in whichever region $t(\Omega_{g^{\pm}})$ contains the basepoint of B.

For any two balls B_1, B_2 that are not tangent there is some isometry in Γ taking their basepoints to different Ω regions. Since $p(B1)$ and $p(B_2)$ are also contained in different regions, $B_1 \cap B_2 = \emptyset$. Since no two balls can intersect in their interiors, no horoball but B_∞ can have radius more than $\frac{1}{2}$. By Proposition 5.4, no element of Γ other than the identity can have representation $\begin{pmatrix} a & b \\ c & d \end{pmatrix} \in PSL(2, \mathbb{C})$ with $|c| < 1$. Therefore the identity element is isolated and Γ is discrete.

□

5.3 Supporting Propositions

To make calculations easier, in the proof of the following Propositions, we often normalize the size and separation of horoballs. As a trick to keep track of the image of where curves in $\mathbb{C}$ go, we look at the hyperbolic distance between horoballs based on the points on these curves and other balls. For example, if ball B_a has basepoint on the circle $C(0, \frac{1}{a})$ and is tangent to the B_0, (the ball at 0 with radius $\frac{1}{2}$), then B_a must have radius $r_a = \frac{1}{2a^2}$ and therefore $d_{hyp}(B_a, B_\infty) = \ln a^2$. If we want to know what happens to this circle under some map ω, then rather than working with ω itself, which can get messy quickly, we can use $\omega(B_0)$ and $\omega(B_\infty)$ as "guideposts".

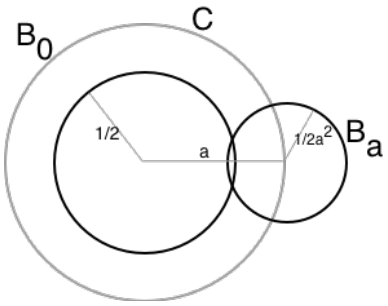

Figure 5.2

The following proposition defines a shortcut for this process and gives us an easy way to keep track of the image of disks.

Proposition 5.1. *Let $\omega(B_\infty) = B_1$, $\omega(B_0) = B_2$, and let C be the circle $C(0, r)$. For $\gamma \in \Gamma$ let $B_1 = \gamma(B_\infty)$ and $B_2 = \gamma(B_0)$. Let ψ be a normalizing function such that $\psi(B_2)$ is centered at 0 and has radius 1 while $\psi(B_1)$ is centered at some point d on the real axis with radius r_1. Then $\psi(\gamma(C))$ has center at $(\frac{2d}{2+d/r} + \frac{2d}{2-d/r})/2$ and radius $(\frac{2d}{2+d/r} - \frac{2d}{2-d/r})/2$.*

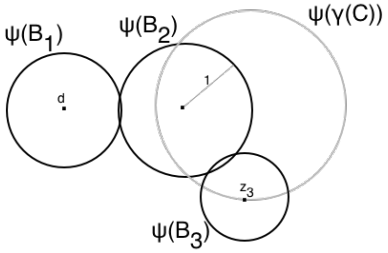

Figure 5.3: A diagram for Proposition 5.1

Proof. For point z_3 on $\psi(\gamma(C))$, let B_3 be the ball based on z_3 that is tangent to B_2. We have $d_{hyp}(B_3, B_1) = \ln(1/r^2)$. If B_3 has radius r_3 we have $|z_3|^2/4 = r_3$, $|d|^2/4 = r_1$, and $\ln(\frac{|z_3-d|^2}{4r_1r_3}) = \ln(1/r^2)$. This has real solutions at $\frac{2d}{2\pm d/r}$. Since the center of the circle $\psi(\omega(C))$ is also real, the center and radius are $(\frac{2d}{2+d/r} + \frac{2d}{2-d/r})/2$ and $(\frac{2d}{2+d/r} - \frac{2d}{2-d/r})/2$, as claimed.

□

Surprisingly, chains of horoballs emanating from B_∞ do not strictly decrease. How-

ever the following proposition gives a bound on the relative size of tangent horoballs. Specifically we say that when moving in the direction of increasing g-number, a sequence of tangent balls can not increase by more than a factor of $1/r^2$ for r dictated by Ω_G.

Proposition 5.2. *Let Ω_G be defined as in Theorem 5.2 for $\Gamma = \langle m, n, g\rangle$. Let $B_1 = \gamma(B_\infty)$ and $B_2 = \gamma(B_0)$ be horoballs with basepoints in Ω_G for $\gamma \in \Gamma$. Let r_1 be the radius of B_1 and r_2 be the radius of B_2. If $D = D(0, r) \subset \Omega_G$, then $r_1 > r^2 r_2$.*

Proof. We show that for $r_1 \leq r^2 r_2$, the image of D under the action of an element of Γ is unbounded in $\mathbb{C}$, which violates Corollary 2.

Normalize as in Proposition 5.1 so B_2 is centered at 0 with radius 1 and B_1 is centered at d on the real axis, take $d > 0$. By Proposition 5.1, $\frac{2d}{2 \pm d/r}$ are points on $\psi(\gamma(\partial(D)))$. Note that $0 \in \psi(\gamma(D))$ and that $\frac{2d}{2 \pm d/r}$ includes the point at ∞ when $d = \pm r$. So for $-2r \leq d \leq 2r$, we have $\infty \in \psi(\gamma(D))$ and therefore $\infty \in \gamma(D)$ as well.

Note that the word γ must begin with G since $B_1 \in \Omega_G$ and $D \subset \Omega_G$. By corollary 2, ∞ cannot be in $\gamma(D)$, therefore $|d| > 2r$. Since $d^2 = 4r_1 r_2$, we have $r_1 > r^2 r_2$.

$r_1 < r^2 r_2$ $\qquad$ $r_1 > r^2 r_2$

Figure 5.4

□

Proposition 5.3. *Let $\Gamma = \langle m, n\rangle * \langle g\rangle$ with m, n parabolic, and let a be the minimum separation of full sized horoballs as above. Further assume that some regions Ω_g and*

Ω_G lie in $\mathbb{C}$ and satisfy Theorem 5.2. With $b = a - 1/2$, let $D_1 = D(0, 1/b)$ and $D_2 = D(g(\infty), 1/b)$ be disks in $\mathbb{C}$. Then for every ball B we have $\gamma \in \Gamma$ such that either $p(B) \subset \gamma(D_1)$ or $p(B) \subset \gamma(D_2)$.

Proof. Let horoball $B_2 = \omega(B_0)$ have basepoint in Ω_G. Let B_1 be the horoball tangent to Ω_G with smaller g-number. Since Γ is free bicuspid this choice is unique. We show that for any ball $B_3 \neq B_1$ that is tangent to B_2, $p(B_3) \subset \omega(D_1)$. The equivalent argument holds for B_2 with basepoint in Ω_g.

We now normalize our picture as in Proposition 5.1 so that B_2 has basepoint at 0 and has radius 1, and ball B_1 has a basepoint at d on the real axis. By Proposition 5.1, we know $\omega(D_1)$ has center and radius as follows. Call $D_\beta = \omega(D_1)$ and $C_\beta = \partial(\omega(D_1))$.

$$c_\beta = \Big(\frac{2d}{2+db} + \frac{2d}{2-db}\Big)/2 \qquad r_\beta = \Big|\frac{2d}{2+db} - \frac{2d}{2-db}\Big|/2$$

We wish to show that for any ball B_3 tangent to B_2, we have $p(\psi(B_3)) \subset \omega(D_1)$. To do this we construct a region R consisting of basepoints z_i for which this is is true. We then show that all balls tangent to B_2 other than B_1 must have basepoints in a disk D_α. Finally we show $D_\alpha \subset R$.

Define $R = \{z_i : \frac{|z_i|^2}{4} + |z_i - c_\beta| \leq r_\beta\}$. If ball B_i has radius r_i, center z_i, and is tangent to B_2, then it must have radius $r_i = \frac{|z_i|^2}{4}$. Observe that if $p(B_i) \subset D_\beta$, then $\frac{|z_i|^2}{4} + |z_i - c_\beta| \leq r_i + |z_i - c_\beta| \leq r_\beta$. Therefore R is as desired.

Any horoball B_i that is tangent to B_2 must have $d_{hyp}(B_i, B_1) \geq \ln(a^2)$. By Proposition 5.1, a disk of basepoints with this property (call it D_α) has center and radius

$$c_\alpha = (\frac{2d}{2+da} + \frac{2d}{2-da})/2 \qquad r_\alpha = |\frac{2d}{2+da} - \frac{2d}{2-da}|/2$$

It suffices to show $D_\alpha \subset R$. Therefore we wish to show:

$$|z_i - c_\alpha| \leq r_\alpha \Rightarrow |z_i|^2/4 + |z_i - c_\beta| \leq r_\beta \tag{13}$$

$$|x + iy - c_\alpha| \leq r_\alpha \Rightarrow |x + iy|^2/4 + |x_i y - c_\beta| \leq r_\beta \tag{14}$$

$$y^2 \leq r_\alpha^2 - (x - c_\alpha)^2 \Rightarrow y^2 \leq 8 + 4r_\beta - x^2 - 4\sqrt{2 + c_\beta^2 + 4r_\beta - 2c_\beta x} \tag{15}$$

Which follows from:

$$r_\alpha^2 - (x - c_\alpha)^2 \leq 8 + 4r_\beta - x^2 - 4\sqrt{2 + c_\beta^2 + 4r_\beta - 2c_\beta x} \tag{16}$$

By substituting $c_\alpha, c_\beta, r_\alpha, r_\beta$, we can see that (16) holds when the zeros of the left are between the zeros of the right. That is:

$$2 - 2\sqrt{1 - c_\beta + r_\beta} \leq c_\alpha - r_\alpha < c_\alpha + r_\alpha \leq -2 + 2\sqrt{1 + c_\beta + r_\beta} \tag{17}$$

$$b \geq \frac{2 - 4a + a^2 d}{-4 + d + 2ad} \quad and \quad b \geq \frac{-2 + 4a + 2a^2 d}{4 + d + ad} \tag{18}$$

Taking $b = a - 1/2$ we have $d(2ad + d - 4) > 0$ and $d(2ad + d + 4) > 0$, which hold for $a > 1$ and $|d| > 1$, completing the proof.

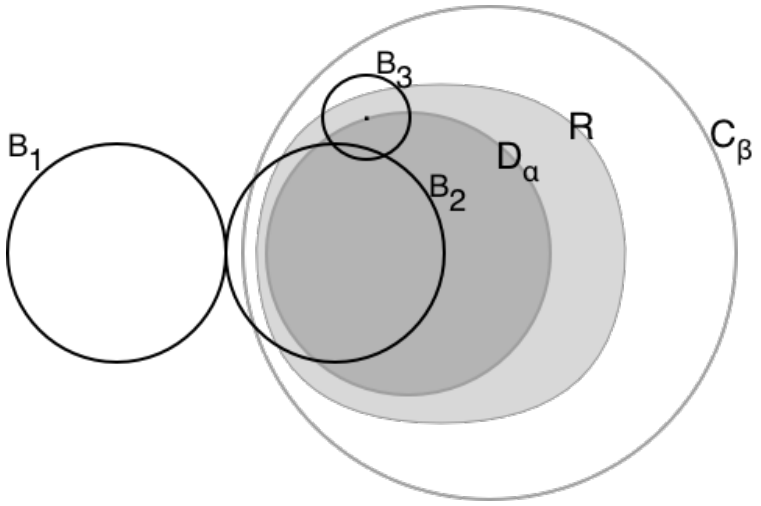

Figure 5.5: R, the region of points z_3 for which the ball B_3 centered at z_3 has $p(B_3) \subset D_\beta$, contains D_α, the collection of possible basepoints under the specified conditions.

□

Note that this b, this requirement of a disk of radius $1/b$, can be improved slightly: we need not require that D_1 covers all $p(B_i)$ balls for any B_i. By Proposition 5.2 we only need to consider balls of radius down to $1/b^2$, therefore this proposition would still hold with a slightly less stringent requirement for b. However $b = a - 1/2$ is more than sufficient for our purposes so we leave Proposition 5.3 as is.

Proposition 5.4. *Let* $\Gamma = \langle m, n, g \rangle$ *where*

$$m = \begin{pmatrix} 1 & A \\ 0 & 1 \end{pmatrix} \quad n = \begin{pmatrix} 1 & B \\ 0 & 1 \end{pmatrix} \quad g = \begin{pmatrix} C & D \\ -1/D & 0 \end{pmatrix}$$

and $|D| = 1$. *Let* w *be a word in* Γ *with representation* $\mathcal{M} = \begin{pmatrix} a_1 & b_1 \\ c_1 & d_1 \end{pmatrix}$ *in* $PSL(2, \mathbb{C})$. *Then the horoball at* $w(\infty)$ *has radius* $\frac{1}{2|c_1|^2}$.

Proof. As parabolic isometries fixing ∞ do not change a horoball's radius, we can assume that w ends in either $G = g^{-1}$ or g. We induct on the g number of the word. First observe that both g and $G =$ have $|c| = 1$.

Assuming that this proposition holds for w, we show that it holds for wtG for $t \in \langle m, n \rangle$. Again, since t preserves horoball radii, we may take $t = 1$.

Let z_1 and r_1 be the basepoint and radius of the w horoball and z_2 be the basepoint for wG. Observe that $w : \infty \mapsto \frac{a_1}{c_1} = z_1$ and $w : 0 \mapsto \frac{b_1}{d_1} = z_2$. Since $a_1 d_1 - b_1 c_1 = 1$, we have $c_1 d_1 = \frac{1}{z0 - z1}$. We have,

$$r_2 = \frac{(z_2 - z_1)^2}{4r_1^2} = \frac{(|\frac{1}{c_1 d_1}|)^2}{4\frac{1}{2|c_1|^2}} = \frac{1}{2|d_1|^2}$$

Now since

$$\begin{pmatrix} a_2 & b_2 \\ c_2 & d_2 \end{pmatrix} = \mathcal{M}G$$
$$= \begin{pmatrix} a_1 & b_1 \\ c_1 & d_1 \end{pmatrix} \begin{pmatrix} 0 & -D \\ 1/D & C \end{pmatrix}$$
$$= \begin{pmatrix} b_1/D & b_1C - a_1D \\ d_1/D & d_1C - c_1D \end{pmatrix}$$

We have $c_2 = d_1/D$, so $|c_2| = |d_1|$. Therefore $r_2 = \frac{1}{2|c_2|^2}$ as claimed. □

6 Constructing Examples

6.1 Defining Γ

In this section we construct a class of manifolds by specifying a group of isometries of $\mathbb{H}^3$. In the spirit of Gabai et. al, we do this by specifying parameters which dictate the size and shape of the cusp. We choose to work with manifolds with maximal cusp diagrams featuring full-sized horoballs in a hexagonal packing (see figure). By making this assumption, we reduce Gabai et. al.'s six parameters to two. A single real parameter a now governs the relative distance of all full-sized horoballs, while another real parameter θ governs the rotational element of the loxodromic transformation. We follow Agol's normalizing convention rather than that of Gabai et. al. as it makes some calculations easier.

Let $\Gamma = \langle m, n, g \rangle$. With

$$m : z \mapsto z + a/2 - a * i\sqrt{3}/2$$

$$n : z \mapsto z + 3a/2 + a * i\sqrt{3}/2$$

$$g : z \mapsto a + \frac{e^{-i\theta}}{z}$$

It is often useful to work with these transformations' representations in $PSL(2,\mathbb{C})$, where

$$m = \begin{pmatrix} 1 & a/2 - a * i\sqrt{3}/2 \\ 0 & 1 \end{pmatrix} \quad n = \begin{pmatrix} 1 & 3a/2 + a * i\sqrt{3}/2 \\ 0 & 1 \end{pmatrix}$$

$$g = \begin{pmatrix} a\exp\left(i(-\theta)/2\right) & \exp\left(i(\theta)/2\right) \\ \exp\left(i(-\theta)/2\right) & 0 \end{pmatrix}$$

The convention is usually to rotate the picture so that the shorter parabolic m corresponds to translation along the real axis. We choose instead to base the Adams horoball ($g(B_\infty)$) on the real axis because it simplifies calculations in Section 6.3. See Figure 6.1.

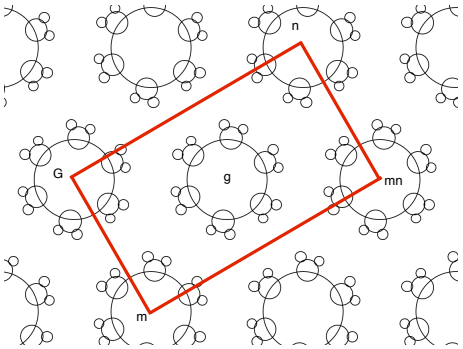

Figure 6.1: a= 1.90952, $\theta = 35.66°$

Our question becomes, for which values a and θ is Γ a free bicuspid torsion-free Kleinian group? We are particularly interested in pairs which minimize a and therefore minimize the cusp size. Typically if a pair (a,θ) yields a free bicuspid Kleinian group, then (a_i,θ) for $a_i > a$, does as well.

6.2 Ford Domains

These examples are inspired by a construction of Ian Agol. In fact if we take $a \geq 2$ and $\theta = 0$, we recover his example. He argues that in this case, I_g and I_G, the isometric spheres for g and G are disjoint on their interior and that the Ford domain constructed by identifying these spheres results in a discrete manifold. A simple

expansion of his argument shows this is true for any value of θ if $a \geq 2$, however with any $a < 2$ this argument falls apart because I_g and I_G must then intersect on their interiors.

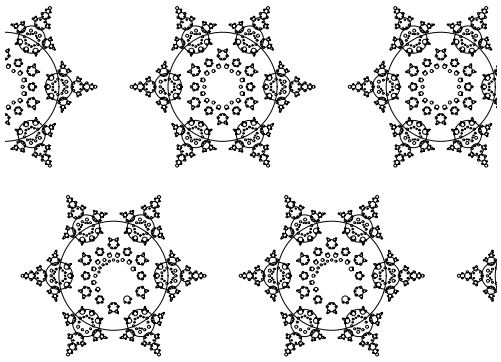

a = 2, $\theta = 0$

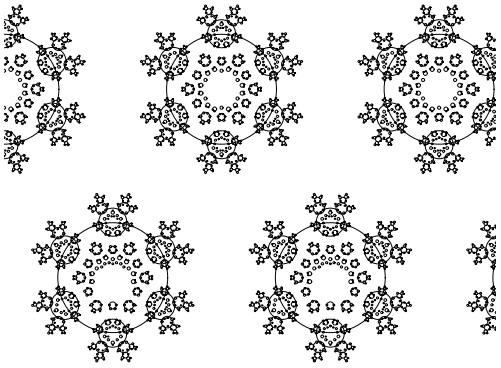

a = 1.96, $\theta = 30°$

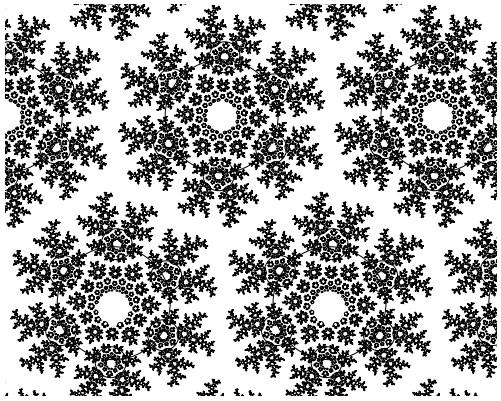

a = 1.9114, $\theta = 32.9°$

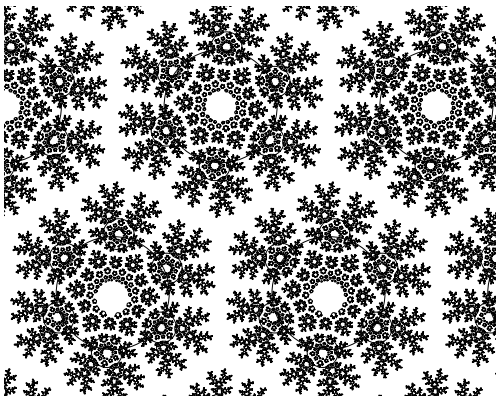

a = 1.90952, $\theta = 35.66°$

Figure 6.2: Maximal Cusp Diagrams

While computationally impractical for the low values of a we wish to analyze, this type of argument could conceivably be generalized for the manifolds we present in this paper. That is, we can construct the Ford domain for the manifold we claim is discrete, then show that each of the face pairings satisfies certain edge conditions. We choose to rely on the theorems in section 5 instead, but it is a worthwhile venture to go through the construction of a Ford domain in a simple case of our defined Γ.

Let $a = 1.98$ and $\theta = \pi/6$. Figure 6.3 shows boundaries of isometric spheres for g and G (the largest circles), as well as the spheres for several other words with g-number 2. Note that I_G intersects I_g and that I_G intersects I_{G^2}. These intersections

form edges, around which we can check the edge condition that the dihedral angles sum to 2π.

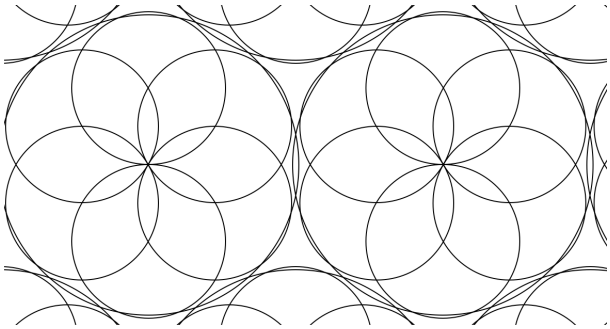

Figure 6.3: Isometric spheres for words with g-number at most 2. $a = 1.96$ $\theta = \pi/6$

Observe that each full-sized isometric sphere (I_G, I_g, and parabolic translates of these) intersects six other full-sized spheres. In the gaps between these intersections, I_{G^2} (and symmetric copies of I_{G^2}) 'poke out' from under I_G. The fact that these two intersections are disjoint makes our calculations far simpler, but this is not required for this construction to hold. These two intersections are illustrated in Figure 6.4.

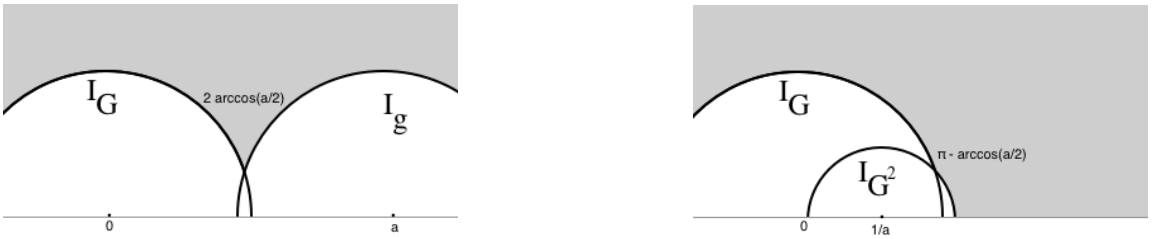

Figure 6.4: Cross sections of Figure 6.3

By looking only at our fundamental region (quotienting out by the parabolics) we have two 24-gons identified to each other (with a $\pi/6$ rotation), and twelve bigons identified in pairs. We have six edges, but thanks to the rotational symmetry, each looks like Figure 6.5. Since all edge conditions are met and face pairings specified, we have a Ford Domain for a Hyperbolic 3-Manifold.

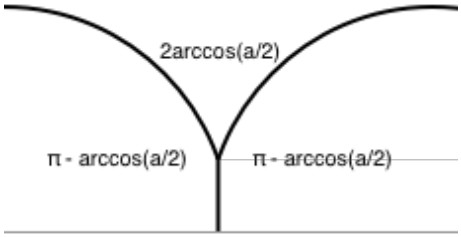

Figure 6.5: The total angle around an edge (seen as the center point in this diagram) sums to 2π.

6.3 Defining Ω

For specific values of a and θ we construct regions Ω_G and Ω_g that meet the following restrictions, which are stronger than the requirements of Theorems 5.2 and 5.3.

1. Ω_G has a 6-fold rotational symmetry around 0
2. $\Omega_g = \Omega_G + a$
3. $\Omega_g \cap \Omega_G = \emptyset$.
4. $G(\Omega_G) \subset \Omega_G$.
5. $D(0, a - 1/2) \subset \Omega_G$

In practice, we define $\partial(\Omega_G)$ as piecewise arcs of circles which are determined by a recursive python script. Appendix B contains descriptions of a number of these boundaries in a format which while unenlightening, can be verified to meet the above requirements with a simple script. We prefer to look at plots of these curves, many of which are also included in Appendix B.

The following is an example of Ω_G, which can be visually checked to meet these above requirements (and therefore the requirements of Theorems 5.2 and 5.3.

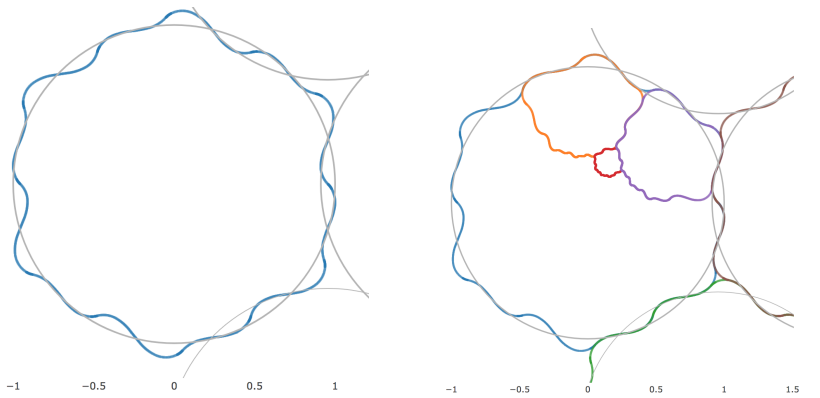

Ω_G

Ω_G in blue, Ω_g in brown, $m\Omega_G$ in green, $G(\Omega_G)$ in purple.

Figure 6.6: $a = 1.9114, \theta = 32.9°$

6.4 How we compute Ω

In this section we briefly discuss the rough idea behind the process in which these Ωs were constructed and how a more refined computational approach would likely yield a better (smaller a) result.

We fix θ, choosing $\pi \leq \theta < 4\pi/3$ so that points in the vicinity of 1 remain in the vicinity of 1. We then make the assumption that a point, say $z_0 = g(a/2), \in \Omega_G$. It follows that $G^n(z_0) \in \Omega_G$. These points limit towards a point in the interior of Ω_G, but we can view the first several of these points as generating a framework for the boundary of Ω_G. The path we choose to connect any pair of these points, say z_0 and $G(z_0) = a/2$, propagates through and dictates how subsequent points are connected. For example, if we naively connect z_0 and $g(z_0)$ with a straight line, subsequent pairs are connected by circle arcs bowing outward, see Figure 6.7.

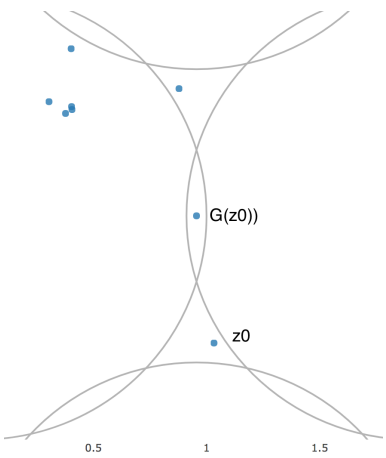

$z_0 = g(a/2)$ and several points $G^n(z_0)$

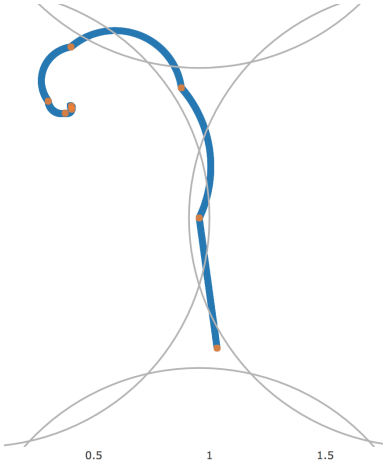

z_0 and $G(z_0)$ connected with a straight line and the image of that line under iterations of G

Figure 6.7: $a = 1.9114, \theta = 32.9°$

Since we are assuming a six-fold rotational symmetry, for $r : z \mapsto ze^{-\pi i/3}$, $r^m G^n(z_0) \in \Omega_G$ as well. With our naive approach this creates a problem: the straight line segment z_0 to $G(z_0)$ is supposed to be a portion of the boundary of Ω, however points that should be in Ω fall outside. See Figure 6.8.

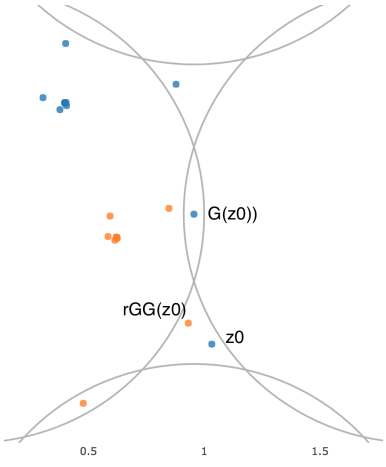

$G^n(z_0)$ in blue and $rG^n(z_0)$ in orange

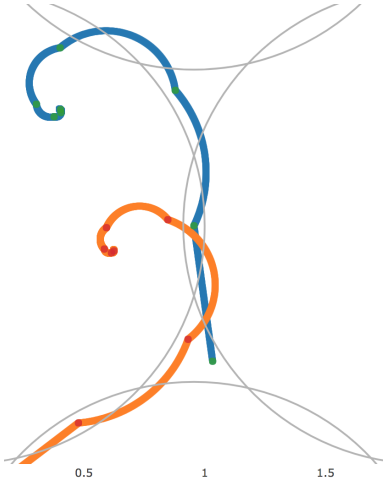

Figure 6.8: $a = 1.9114, \theta = 32.9°$

To remedy this we choose to connect z_0 and $G(z_0)$ with a path that includes the relevant points $rG^n(z_0)$. In this case, point $rGG(z_0)$. Depending on the separation

a, this is not always possible: not only must a continuous path join z_0 to $rGG(z_0)$ to $G(z_0)$, but it must also avoid its own image under rGG. For values of a below a certain threshold any such path will create new obstructions quicker than it avoids them. This threshold is dependent on the relative vectors of rGG and G at a particular point, as well as the location of the limit point of the $(rGG)^n(z_0)$.

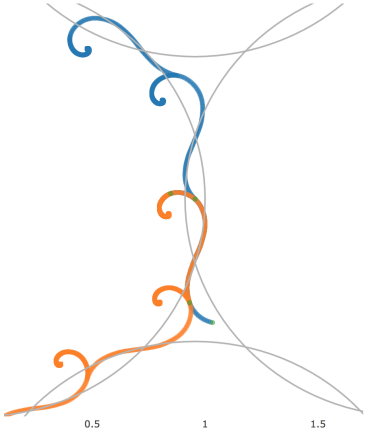

The spirals are artifacts of limit points for maps such as rGG. These are discarded when defining Ω_G.

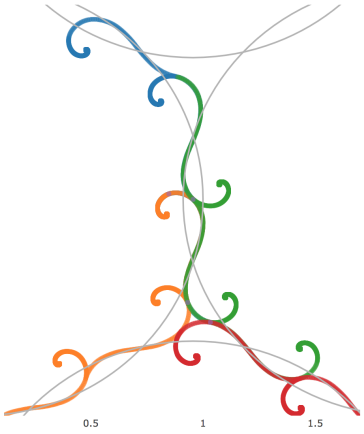

The red and green curves are a portion of Ω_g, illustrating that the boundary of these regions is shared.

Figure 6.9: $a = 1.9114, \theta = 32.9°$

For a slightly above this threshold, we can recursively define a path to meet our needs, see Figure 6.9. These graphics show the boundary of Ω as well as its own image under iterated transformations such as G and rGG. As such, these graphics include spirals around limit points of these transformations. When we define $\partial\Omega$ itself we omit these spiraling tails. Figure 6.10 shows the final version of the case we have been working on in this section.

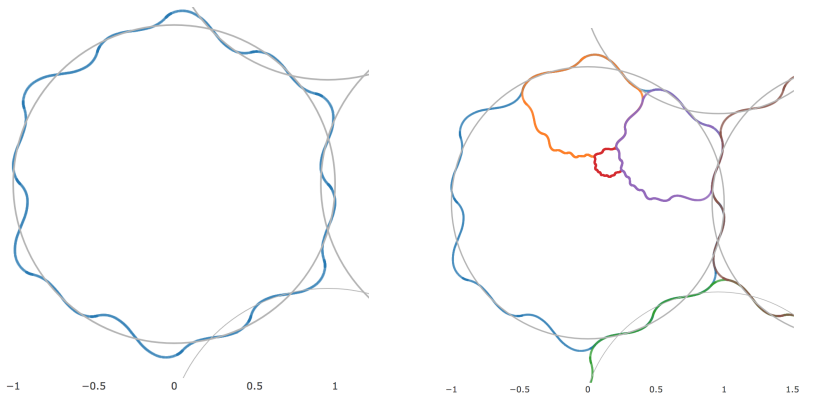

Ω_G

Ω_G in blue, Ω_g in brown, $m\Omega_G$ in green, $G(\Omega_G)$ in purple.

Figure 6.10: $a = 1.9114, \theta = 32.9°$

6.5 Iterating Further

In the previous example we drew the boundary of Ω_G using the points $(rGG)^n(z_0)$ as guideposts. We chose the rGG transformation because $rGG(z_0)$ is "close" to z_0 for our given θ. We can take this a step further and use observations about words ω in r and G for which $\omega(z_0) \approx z_0$.

The best (smallest a) example we have constructed to date uses this approach, observing that for $a = 1.90952$ and $\theta = 180 + 35.66°$, we have $rG(rGG)^3g(a/2) \approx g(a/2)$, see Figure 6.12. We are not however looking for words where this is exactly true. In practice if we find a word ω with $\omega(z_0) = z_0$, then a can be slightly reduced by perturbing θ slightly so that $\omega(z_0) = z_0$.

6.6 Ω and Γ

We construct these regions Ω in the first place to show that a maximal cusp diagram is bounded under repeated iterations of G and its conjugates. Figures 6.11 and 6.12 illustrate this bounding region in action. We see how the fractal nature of the maximal cusp diagram can be segregated with these bounding regions.

One feature of the Ω regions worth pointing out is the triangle of "unused" space where three regions meet. In Figure 6.11, the blue, green, and yellow regions leave

this triangle between them. As mentioned in Section 1, an infinite-volume cusped hyperbolic 3-manifold must be free bicuspid. While the converse is not necessarily true, all of the examples we construct feature a portion of the bounding plane $\hat{\mathbb{C}}$ not covered by the isometric spheres corresponding to elements of Γ. In other words, all our examples have this unused triangle and are therefore of infinite volume.

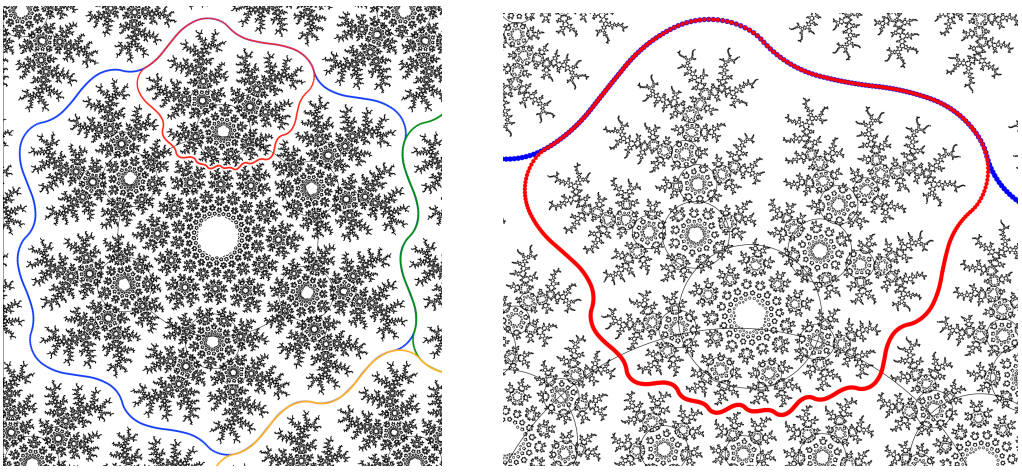

≈2x magnification of the image on the left

Figure 6.11: The maximal cusp diagram for $a = 1.9114, \theta = 32.9°$, together with Ω_G in blue, Ω_g in green, and $Gm(\Omega_G)$ in red.

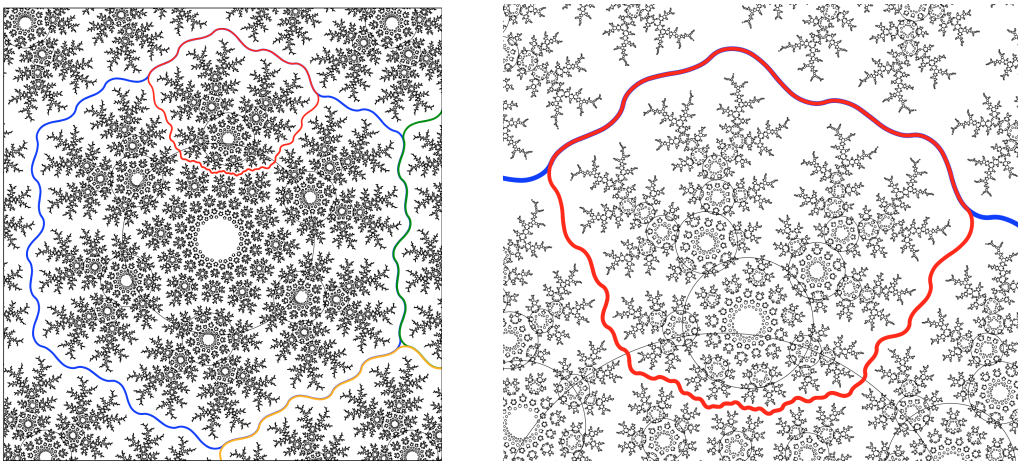

≈2x magnification of the image on the left

Figure 6.12: The maximal cusp diagram for $a = 1.90952, \theta = 35.66°$, together with Ω_G in blue, Ω_g in green, and $Gm(\Omega_G)$ in red.

7 Discussion and Future Work

7.1 Potential Improvement

Recall that our primary goal is to find the infinite-volume hyperbolic 3-manifold that minimizes cusp volume. For the examples above which feature a parabolic subgroup generating a hexagonal packing of separation a, the cusp volume is $a^2\sqrt{3}/2$. Therefore the example with $a = 1.90952$ has cusp volume ≈ 3.15776, a significant improvement over the previous minimum of 3.238 when considering Agol's lower bound of π.

In section 6.5 we discuss using an additional level of recursion to define $\partial(\Omega_G)$. The word to iterate over in the second level of recursion was chosen somewhat by hand, using a guess and check approach to find suitable words and values of a and θ. A more refined algorithm could accomplish this far more efficiently. At the moment the biggest hurdle is devising a suitable measure of when a cannot be reduced any further without "breaking" the system. More research is needed to understand how various tangent vectors of various transformations impact this minimum value of a.

That said, we conjecture that the methods introduced can be refined to construct examples of free bicuspid manifolds with cusp volume arbitrarily close to the bound of π, thus showing that the bound is sharp.

We decided early on to work in the case where P forms a hexagonal lattice. Since the goal is to minimize cusp size, we want the full-sized horoballs to start as close to each other as possible. It is entirely possible that an improvement could be made by relaxing this restriction. The example Agol found in the SnapPy census, figure 4.1, has a slightly off kilter hexagonal packing. This shifting contributes, in addition to the rotational element of g, to the curvature of the 'arms' of the horoball chains in ways that are not well understood.

7.2 Elder Sibling Property

Freedman and McMullen introduced the *Elder Sibling Property* of a maximal cusp diagram as a way of determining tameness of a manifold. Such a diagram has the Elder Sibling Property if there is a horoball B_1 such that every other ball B_i is connected to B_1 by a finite chain moving monotonically closer to B_1. This is equivalent to the property that every horoball is tangent to a ball of greater radius.

At first glance the manifolds we construct in Section 6 appear to have this property: moving outward from B_0 the balls appear to monotonically decrease. Surprisingly, these manifolds do not have this property and we can identify chains that briefly increase in horoball radius before again decreasing.

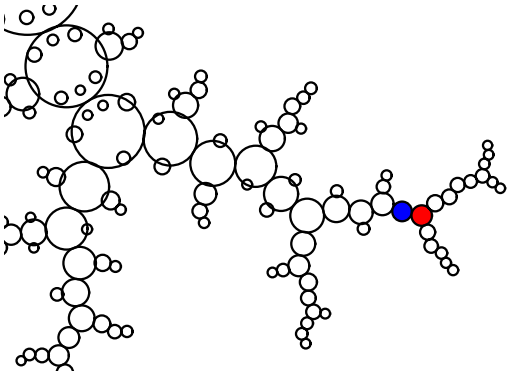

Figure 7.1: The blue horoball has radius .00214469 while red has radius .00223841

Figure 7.1 illustrates a horoball (blue) with g-number 18 tangent to a larger ball (red) with g-number 19, the earliest (in terms of g-number) example of an increase in radius that we found.

By Proposition 5.2 we have a bound on the relative size of a pair of tangent horoballs, and by the discreteness we know any chain can only have a finite number of horoballs above any radius bound. Other than this we do not know much about the behavior of these sequences. Examples can be constructed which feature chains with a seemingly arbitrary number of size increases before an eventual size decrease.

As especially evident in Figure 6.11, these maximal cusp diagrams exhibit a fractal evolving symmetry. Understanding this behavior may yield further insights into these

manifolds, particularly in the case of an 'optimal' example meeting the π bound on cusp volume.

7.3 Parameter Space Boundary

One motivation for the study of these manifolds is their relationship to the parameter space of Gabai et. al. For the region of this space they study (out to cusp volume 2.62) and further (out to cusp volume π), any manifold must have finite volume. As such, no two points in this region correspond to diffeomorphic manifolds. If we look at the parameter points corresponding to the free bicuspid manifolds we construct this is no longer true: we can find open neighborhoods of points in the parameter space all corresponding to hyperbolic 3-manifolds. Some boundary in the parameter space separates these two regions, we are particularly interested in understanding this boundary.

Cast in terms of the a and θ we have been working with, there is some function $f(\theta)$ which returns the minimum a for which the manifold constructed using a, and θ is free bicuspid. Points in the Gabai et. al. parameter space correspond to a deformable infinite-volume free bicuspid manifold exactly when $a > f(\theta)$.

We know that $\sqrt{\frac{2\pi}{\sqrt{3}}} \leq f(\theta) \leq 2$, that f is continuous, and that $f(0) = 2$. However beyond that all we have is conjecture. With minimal data available, we hypothesize that the behavior of this function is comparable to Figure 7.2, notably that peaks occur at θ near rational fractions of π.

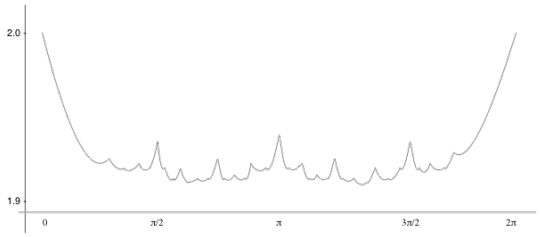

Figure 7.2: A conjecture of the shape of the function returning the minimum value of a given θ

Determining this function f would be a more complete solution than the primary goal of finding the manifold that minimizes a; of determining the smallest possible cusp volume of an infinite-volume manifold.

References

[Ada87] C. Adams. The noncompact hyperbolic 3-manifold of minimal volume. *Proceedings of the American Mathematical Society*, 100:601–606, 1987.

[Ada02] C. Adams. Waist size for cusps in hyperbolic 3-manifolds. *Topology*, 41(2):257–270, 2002.

[Ada17] C. Adams. Waist size for cusps in hyperbolic 3-manifolds ii. arxiv.org/pdf/1703.01324, 2017.

[Ago00] I. Agol. Bounds on exceptional dehn filling. *Geom. Topol.*, 4:431–449, 2000.

[Ago04] I. Agol. Tameness of hyperbolic 3-manifolds. arXiv:math/0405568, 2004.

[Ago10] I. Agol. Bounds on exceptional dehn filling ii. *Geom. Topol.*, 14:1921–1940, 2010.

[AK12] C. Adams and K. Knudson. Unknotting tunnels in hyperbolic 3-manifolds. arXiv:1205.5239, 2012.

[BBP+17] B. Burton, R. Budney, W. Pettersson, et al. Regina: Software for low-dimensional topology. `regina-normal.github.io/`, 1999-2017.

[Bea80] A. Beardon. *Graduate Texts in Mathematics: The Geometry of Discrete Groups*. Springer-Verlag, 1980.

[BH96] S. Bleiler and C. Hodgson. Spherical space forms and dehn filling. *Topology*, 35:809–833, 1996.

[BPZ86] S. Betley, J. H. Przytcki, and T. Zukowski. Hyperbolic structures on dehn filling of some punctured-torus bundles over s^1. *Kobe J. Math*, 3:117–147, 1986.

[CDGW] M. Culler, N. Dunfield, M. Goerner, and J. Weeks. SnapPy, a computer program for studying the geometry and topology of 3-manifolds. snappy.computop.org.

[CM01] C. Cao and R. Meyerhoff. The orientable cusped hyperbolic 3-manifolds of minimum volume. *Invent. math*, 146:451–478, 2001.

[GHM+] D. Gabai, R. Haraway, R. Meyerhoff, N. Thurston, and A. Yarmola. Hyperbolic 3-manifolds of low cusp volume. *In Preparation.*

[GMM11] D. Gabai, R. Meyerhoff, and P. Milley. Mom technology and volumes of hyperbolic 3-manifolds. *Comment. Math. Helv.*, 86:145?188, 2011.

[Goo] O. Goodman. Snap. www.ms.unimelb.edu.au/.

[Gor98] C. Gordon. Boundary slopes of punctured tori in 3-manifolds. *Trans. Amer. Math. Soc.*, 350(5):1713–1790, 1998.

[GT87] M. Gromov and W. Thurston. Pinching constants for hyperbolic manifolds. *Invent. Math*, 89:1–12, 1987.

[Har] R. Haraway. Determining hyperbolicity of compact orientable 3-manifolds with torus boundary. arxiv.org/abs/1410.7115.

[Har00] P. De La Harpe. *Topics in Geometric Group Theory.* University of Chicago Press, 2000.

[HIK+99] N. Hoffman, K. Ichihara, M. Kashiwagi, H. Masai, S. Oishi, and A. Takayasu. Hikmot. arXiv:1310.3410, 1999.

[Lac00] M Lackenby. Word hyperbolic dehn surgery. *Invent. math*, 140:243–282, 2000.

[Lic62] W. Lickorish. A representation of orientable combinatorial 3-manifolds. *Annals of Math*, 76(3):531–540, 1962.

[LM08] M. Lackenby and R. Meyerhoff. The maximal number of exceptional dehn surgeries. arXiv:0808.1176, 2008.

[Mar74] A. Marden. The geometry of finitely generated kleinian groups. *Annals of Mathematics*, 99:383–462, 1974.

[Mar07] A. Marden. *Outer Circles.* Cambridge, 2007.

[Mey96] R. Meyerhoff. The ortho-length spectrum for hyperbolic 3-manifolds. *Quarterly Journal of Mathematics*, 47(3):349–359, Sept 1996.

[Mos68] G. Mostow. Quasi-conformal mappings in n-space and the rigidity of hyperbolic space forms. *Publications Math'ematiques De L'IHES'*, 34:53–104, 1968.

[MP02] B. Martelli and C. Petronio. Dehn filling of the magic 3-manifold. *Comm. Anal. Geom.*, 14(5):969?1026, 2002.

[Per02] G. Perelman. The entropy formula for the ricci flow and its geometric applications, 2002.

[Pra73] G. Prasad. Strong rigidity of q-rank 1 lattices. *Invent. math.*, 21:255–286, 1973.

[Thu97] W. Thurston. Three-dimensional geometry and topology. *Princeton University Press*, 1997.

[W.T78] W.Thurston. The geometry and topology of 3-manifolds. *Lecture notes from Princeton University*, 1978.

A Non-Hyperbolic Manifolds

In Section 3.1 we use Haraway's Regina script to show the following 69 manifolds are not hyperbolic.

Manifold	Cusp	Surgeries
s782	0	[(1, 0), (0, 1), (1, 1), (-1, 1), (-2, 1)]
s782	1	[(1, 0), (0, 1), (1, 1), (-1, 1), (-2, 1)]
v2124	0	[(1, 0), (0, 1), (1, 1), (-1, 1)]
v2124	1	[(1, 0), (0, 1), (1, 1), (-1, 1)]
v2355	0	[(1, 0), (0, 1), (1, 1), (-1, 1)]
v2355	1	[(1, 0), (0, 1), (1, 1), (-1, 1)]
v2533	0	[(1, 0), (0, 1), (1, 1), (-1, 1)]
v2533	1	[(1, 0), (0, 1), (1, 1), (-1, 1)]
v2644	0	[(1, 0), (0, 1), (-1, 1)]
v2644	1	[(1, 0), (0, 1), (-1, 1)]
v2731	0	[(1, 0), (0, 1), (-1, 1)]
v2731	1	[(1, 0), (0, 1), (1, 1), (-1, 1)]
v3108	0	[(1, 0), (0, 1), (1, 1), (-1, 1)]
v3108	1	[(1, 0), (0, 1), (1, 1), (-1, 1)]
v3127	0	[(1, 0)]
v3127	1	[(1, 0)]
v3211	0	[(1, 0), (0, 1), (-1, 1)]
v3211	1	[(1, 0), (0, 1), (-1, 1)]
v3376	0	[(1, 0), (0, 1), (-1, 1)]
v3376	1	[(1, 0), (0, 1), (-1, 1)]

The following table shows what fault the script found, with T^2 an essential Torus, K^2 a Klein Bottle, D^2 a disk, M^2 a mobius band, S^2 an essential sphere, and π_1 a fault with the fundamental group, indicating that the manifold is Seifert Fibred.

	s782		v2124		v2355		v2355	
Surgery	Cusp 0	Cusp 1	Cusp 0	Cusp 1	Cusp 0	Cusp 1	Cusp 0	Cusp 1
(1,0)	K^2	K^2	T^2	T^2	T^2	T^2	D^2	T^2
(0,1)	M^2	K^2	π_1	π_1	π_1	π_1	π_1	π_1
(1,1)	T^2	T^2	D^2	D^2	T^2	T^2	T^2	π_1
(-1,1)	π_1	π_1	T^2	T^2	M^2	M^2	T^2	M^2
(-2,1)	T^2	T^2	-	-	-	-	-	-

	v2644		v2731		v3108		v3127	
Surgery	Cusp 0	Cusp 1	Cusp 0	Cusp 1	Cusp 0	Cusp 1	Cusp 0	Cusp 1
(1,0)	D^2	D^2	D^2	M^2	T^2	T^2	D^2	D^2
(0,1)	π_1	π_1	T^2	T^2	π_1	π_1	-	-
(1,1)	-	-	-	T^2	M^2	M^2	-	-
(-1,1)	T^2	T^2	T^2	π_1	T^2	T^2	-	-

	v3211		v3376	
Surgery	Cusp 0	Cusp 1	Cusp 0	Cusp 1
(1,0)	D^2	D^2	D^2	D^2
(0,1)	π_1	π_1	T^2	T^2
(1,1)	T^2	T^2	T^2	T^2

Table A.1: Faults found in the 69 manifolds

B Representing $\partial(\Omega_G)$

In our constructions, $\partial(\Omega_G)$ is a collection of piecewise arcs of circles. We usually use python and plot.ly to plot $\partial(\Omega_G)$, but here we include list representations of $\partial(\Omega_G)$ for two of our constructed manifolds. Thanks to the 6-fold symmetry, it suffices to check that $\Omega_G \cap \Omega_G + a = \emptyset$ and $g(\Omega_G) \subset \Omega_G$. This can by checked with a simple python script, or seen visually by inspecting the plots of the regions. To recover $\partial(\Omega_G)$ from the following tables, connect points A and B with the circle arc that passes through point B.

Point A	Point B	Point C
-0.9557+0j	-0.921507434215-0.0522178891333j	-0.910917311955-0.111208462829j
-0.910917311955-0.111208462829j	-0.917270724886-0.16722294347j	-0.932908443796-0.218552569978j
-0.932908443796-0.218552569978j	-0.952384151671-0.267473043286j	-0.971637978543-0.317586806567j
-0.971637978543-0.317586806567j	-0.986095987609-0.372557420965j	-0.98862643006-0.4343808651j
-0.98862643006-0.4343808651j	-0.969040831956-0.499096855243j	-0.920569693123-0.551157082712j
-0.920569693123-0.551157082712j	-0.900036228789-0.562126787399j	-0.878539148827-0.568352464111j
-0.878539148827-0.568352464111j	-0.816973948052-0.591816854923j	-0.769361696744-0.628430645646j
-0.769361696744-0.628430645646j	-0.731960323136-0.669505492243j	-0.699205251298-0.711286214123j
-0.699205251298-0.711286214123j	-0.665747375175-0.752066743949j	-0.626553889681-0.789731529867j
-0.626553889681-0.789731529867j	-0.577434899908-0.819516717621j	-0.518011510594-0.832478045621j
-0.518011510594-0.832478045621j	-0.497575912752-0.831803511516j	-0.47785-0.827660478397j
-0.47785-0.827660478397j	-0.415531698586-0.824157792373j	-0.359149302052-0.844481764315j
-0.359149302052-0.844481764315j	-0.313816045302-0.877991221634j	-0.277182144235-0.917198696721j
-0.277182144235-0.917198696721j	-0.244553625522-0.958525391152j	-0.210780746878-1.00025657598j
-0.210780746878-1.00025657598j	-0.17040380288-1.04026288632j	-0.118128350936-1.07336603583j
-0.118128350936-1.07336603583j	-0.0522898603889-1.0887624054j	0.0170311885429-1.07281528155j
0.0170311885429-1.07281528155j	0.0367979636407-1.06051763216j	0.0529380978097-1.04501345316j
0.0529380978097-1.04501345316j	0.104041456725-1.0034286207j	0.159556055274-0.980502096902j
0.159556055274-0.980502096902j	0.213828602688-0.96864898052j	0.266389305143-0.961172617145j
0.266389305143-0.961172617145j	0.318435218014-0.952587511379j	0.370650622194-0.937477350238j
0.370650622194-0.937477350238j	0.421004846332-0.909831651163j	0.461941380303-0.864850150438j
0.461941380303-0.864850150438j	0.471575015554-0.846815136512j	0.47785-0.827660478397j
0.47785-0.827660478397j	0.505975735629-0.77193990324j	0.551768009904-0.733273301486j
0.551768009904-0.733273301486j	0.603454679584-0.710768278164j	0.655726299561-0.698646126744j
0.655726299561-0.698646126744j	0.707830526149-0.691052347866j	0.760857231665-0.682669769417j
0.760857231665-0.682669769417j	0.815692184729-0.667705465357j	0.870498079124-0.638985170735j
0.870498079124-0.638985170735j	0.916750971567-0.589665550157j	0.937600881666-0.521658198843j
0.937600881666-0.521658198843j	0.93683419243-0.498390844758j	0.931477246637-0.476660989048j
0.931477246637-0.476660989048j	0.921015404778-0.411611765782j	0.928917752018-0.352071451256j
0.928917752018-0.352071451256j	0.945788925824-0.299143488277j	0.965594556441-0.249886403022j
0.965594556441-0.249886403022j	0.984182593189-0.20052076743j	0.997204511875-0.14774582037j
0.997204511875-0.14774582037j	0.99843974624-0.0903149335418j	0.979952890898-0.0323721048171j
0.979952890898-0.0323721048171j	0.969150928306-0.0150116249964j	0.9557+0j
0.9557+0j	0.921507434215+0.0522178891333j	0.910917311955+0.111208462829j
0.910917311955+0.111208462829j	0.917270724886+0.16722294347j	0.932908443796+0.218552569978j
0.932908443796+0.218552569978j	0.952384151671+0.267473043286j	0.971637978543+0.317586806567j
0.971637978543+0.317586806567j	0.986095987609+0.372557420965j	0.98862643006+0.4343808651j
0.98862643006+0.4343808651j	0.969040831956+0.499096855243j	0.920569693123+0.551157082712j
0.920569693123+0.551157082712j	0.900036228789+0.562126787399j	0.878539148827+0.568352464111j
0.878539148827+0.568352464111j	0.816973948052+0.591816854923j	0.769361696744+0.628430645646j
0.769361696744+0.628430645646j	0.731960323136+0.669505492243j	0.699205251298+0.711286214123j
0.699205251298+0.711286214123j	0.665747375175+0.752066743949j	0.626553889681+0.789731529867j
0.626553889681+0.789731529867j	0.577434899908+0.819516717621j	0.518011510594+0.832478045621j
0.518011510594+0.832478045621j	0.497575912752+0.831803511516j	0.47785+0.827660478397j
0.47785+0.827660478397j	0.415531698586+0.824157792373j	0.359149302052+0.844481764315j
0.359149302052+0.844481764315j	0.313816045302+0.877991221634j	0.277182144235+0.917198696721j
0.277182144235+0.917198696721j	0.244553625522+0.958525391152j	0.210780746878+1.00025657598j
0.210780746878+1.00025657598j	0.17040380288+1.04026288632j	0.118128350936+1.07336603583j
0.118128350936+1.07336603583j	0.0522898603889+1.0887624054j	-0.0170311885429+1.07281528155j
-0.0170311885429+1.07281528155j	-0.0367979636407+1.06051763216j	-0.0529380978097+1.04501345316j
-0.0529380978097+1.04501345316j	-0.104041456725+1.0034286207j	-0.159556055274+0.980502096902j
-0.159556055274+0.980502096902j	-0.213828602688+0.96864898052j	-0.266389305143+0.961172617145j
-0.266389305143+0.961172617145j	-0.318435218014+0.952587511379j	-0.370650622194+0.937477350238j
-0.370650622194+0.937477350238j	-0.421004846332+0.909831651163j	-0.461941380303+0.864850150438j
-0.461941380303+0.864850150438j	-0.471575015554+0.846815136512j	-0.47785+0.827660478397j
-0.47785+0.827660478397j	-0.505975735629+0.77193990324j	-0.551768009904+0.733273301486j
-0.551768009904+0.733273301486j	-0.603454679584+0.710768278164j	-0.655726299561+0.698646126744j
-0.655726299561+0.698646126744j	-0.707830526149+0.691052347866j	-0.760857231665+0.682669769417j
-0.760857231665+0.682669769417j	-0.815692184729+0.667705465357j	-0.870498079124+0.638985170735j
-0.870498079124+0.638985170735j	-0.916750971567+0.589665550157j	-0.937600881666+0.521658198843j
-0.937600881666+0.521658198843j	-0.93683419243+0.498390844758j	-0.931477246637+0.476660989048j
-0.931477246637+0.476660989048j	-0.921015404778+0.411611765782j	-0.928917752018+0.352071451256j
-0.928917752018+0.352071451256j	-0.945788925824+0.299143488277j	-0.965594556441+0.249886403022j
-0.965594556441+0.249886403022j	-0.984182593189+0.20052076743j	-0.997204511875+0.14774582037j
-0.997204511875+0.14774582037j	-0.99843974624+0.0903149335418j	-0.979952890898+0.0323721048171j
-0.979952890898+0.0323721048171j	-0.969150928306+0.0150116249964j	-0.9557+0j

Table B.1: a=1.9114, $\theta = 32.9$

Point A	Point B	Point C
-0.95476+0j	-0.937920048477-0.0180575412756j	-0.923613678268-0.0372091614013j
-0.923613678268-0.0372091614013j	-0.923613678268-0.0372091614013j	-0.913161091145-0.0603207820789j
-0.913161091145-0.0603207820789j	-0.910978793482-0.0890447612858j	-0.921344501609-0.114295563275j
-0.921344501609-0.114295563275j	-0.921483238954-0.114618721513j	-0.933094226343-0.138176975011j
-0.933094226343-0.138176975011j	-0.93676402401-0.164348500893j	-0.935348050588-0.187601846011j
-0.935348050588-0.187601846011j	-0.935348050588-0.187601846011j	-0.932100684254-0.210011738301j
-0.932100684254-0.210011738301j	-0.931887076917-0.211614549519j	-0.929131574817-0.234278824754j
-0.929131574817-0.234278824754j	-0.929131574817-0.234278824754j	-0.92928337326-0.25808129054j
-0.92928337326-0.25808129054j	-0.93616630822-0.284359012773j	-0.95186889951-0.306047107676j
-0.95186889951-0.306047107676j	-0.952069499682-0.30634051749j	-0.967755068641-0.328770913154j
-0.967755068641-0.328770913154j	-0.973462252784-0.356986623239j	-0.970939240074-0.382619247377j
-0.970939240074-0.382619247377j	-0.970939240074-0.382619247377j	-0.964214804573-0.406628931574j
-0.964214804573-0.406628931574j	-0.963674610102-0.40831549032j	-0.955232259273-0.431679728717j
-0.955232259273-0.431679728717j	-0.955232259273-0.431679728717j	-0.947360633843-0.456120022774j
-0.947360633843-0.456120022774j	-0.942598179312-0.485190830779j	-0.945779688277-0.515006729562j
-0.945779688277-0.515006729562j	-0.945792050445-0.515414475223j	-0.94540689021-0.547532610699j
-0.94540689021-0.547532610699j	-0.927879066782-0.577120227822j	-0.927879066782-0.577120227822j
-0.927879066782-0.577120227822j	-0.903648495482-0.5947834448j	-0.903648495482-0.5947834448j
-0.903648495482-0.5947834448j	-0.876091209976-0.605194442194j	-0.850989481731-0.610597561631j
-0.850989481731-0.610597561631j	-0.850989481731-0.610597561631j	-0.826534282324-0.614968390544j
-0.826534282324-0.614968390544j	-0.82480358237-0.615343847783j	-0.800648368168-0.621525157911j
-0.800648368168-0.621525157911j	-0.800648368168-0.621525157911j	-0.777188358144-0.632156476879j
-0.777188358144-0.632156476879j	-0.755606428497-0.651206898373j	-0.744023920514-0.676006197396j
-0.744023920514-0.676006197396j	-0.743870120248-0.676326627149j	-0.732938974747-0.700769517562j
-0.732938974747-0.700769517562j	-0.713623267219-0.719869175207j	-0.693085626398-0.731901869408j
-0.693085626398-0.731901869408j	-0.693085626398-0.731901869408j	-0.672080037235-0.740847672207j
-0.672080037235-0.740847672207j	-0.670585158335-0.741464088435j	-0.649553939149-0.749856732839j
-0.649553939149-0.749856732839j	-0.649553939149-0.749856732839j	-0.628707964842-0.760257136443j
-0.628707964842-0.760257136443j	-0.607877657406-0.776521037391j	-0.593281105102-0.798355574182j
-0.593281105102-0.798355574182j	-0.593070610531-0.798637303367j	-0.576385628606-0.820239670927j
-0.576385628606-0.820239670927j	-0.550418784084-0.832711735316j	-0.525177239893-0.835215339671j
-0.525177239893-0.835215339671j	-0.525177239893-0.835215339671j	-0.501438265236-0.832401469697j
-0.501438265236-0.832401469697j	-0.47738-0.826846414517j	-0.453321734764-0.821291359337j
-0.453321734764-0.821291359337j	-0.429582760107-0.818477489364j	-0.429582760107-0.818477489364j
-0.429582760107-0.818477489364j	-0.404341215916-0.820981093718j	-0.378374371394-0.833453158107j
-0.378374371394-0.833453158107j	-0.361689389469-0.855055525667j	-0.361478894898-0.855337254852j
-0.361478894898-0.855337254852j	-0.346882342594-0.877171791643j	-0.326052035158-0.893435692591j
-0.326052035158-0.893435692591j	-0.305206060851-0.903836096195j	-0.305206060851-0.903836096195j
-0.305206060851-0.903836096195j	-0.284174841665-0.912228740599j	-0.282679962765-0.912845156828j
-0.282679962765-0.912845156828j	-0.261674373602-0.921790959627j	-0.261674373602-0.921790959627j
-0.261674373602-0.921790959627j	-0.241136732781-0.933823653828j	-0.221821025253-0.952923311472j
-0.221821025253-0.952923311472j	-0.210889879752-0.977366201886j	-0.210736079486-0.977686631638j
-0.210736079486-0.977686631638j	-0.199153571503-1.00248593066j	-0.177571641856-1.02153635216j
-0.177571641856-1.02153635216j	-0.154111631832-1.03216767112j	-0.154111631832-1.03216767112j
-0.154111631832-1.03216767112j	-0.12995641763-1.03834898125j	-0.128225717676-1.03872443849j
-0.128225717676-1.03872443849j	-0.103770518269-1.0430952674j	-0.103770518269-1.0430952674j
-0.103770518269-1.0430952674j	-0.0786687900243-1.04849838684j	-0.0511115045179-1.05890938423j
-0.0511115045179-1.05890938423j	-0.0268809332178-1.07657260121j	-0.0265339962008-1.07678717999j
-0.0265339962008-1.07678717999j	0.00147370516033-1.09251268918j	0.035861244941-1.09212695738j
0.035861244941-1.09212695738j	0.035861244941-1.09212695738j	0.0632733252059-1.07997427558j
0.0632733252059-1.07997427558j	0.0632733252059-1.07997427558j	0.0860681561816-1.06131446497j
0.0860681561816-1.06131446497j	0.103298258996-1.04227729035j	0.103298258996-1.04227729035j
0.103298258996-1.04227729035j	0.119311107573-1.02328388086j	0.120501613057-1.02197277936j
0.120501613057-1.02197277936j	0.137932391758-1.00414440529j	0.137932391758-1.00414440529j
0.137932391758-1.00414440529j	0.158869389072-0.989143100118j	0.186158502862-0.979977811528j
0.186158502862-0.979977811528j	0.213426579804-0.982346714886j	0.213780980243-0.982373734825j
0.213780980243-0.982373734825j	0.240414717033-0.985128530336j	0.266613359521-0.977950465747j
0.266613359521-0.977950465747j	0.287302798786-0.966180694162j	0.287302798786-0.966180694162j
0.287302798786-0.966180694162j	0.305552885848-0.952462221725j	0.306834157411-0.951475826736j
0.306834157411-0.951475826736j	0.324618010263-0.937458578851j	0.324618010263-0.937458578851j
0.324618010263-0.937458578851j	0.344048011147-0.924605637337j	0.368548116251-0.914698012402j
0.368548116251-0.914698012402j	0.394755655944-0.912974295695j	0.39510488786-0.912932866642j
0.39510488786-0.912932866642j	0.422155577912-0.909284432213j	0.445940124771-0.893032517395j
0.445940124771-0.893032517395j	0.460729081839-0.872424501072j	0.460729081839-0.872424501072j
0.460729081839-0.872424501072j	0.470161686287-0.850459010973j	0.47738-0.826846414517j
0.47738-0.826846414517j	0.484598313713-0.803233818062j	0.494030918161-0.781268327962j
⋮	⋮	⋮

Point A	Point B	Point C
0.494030918161-0.781268327962j	0.494030918161-0.781268327962j	0.508819875229-0.760660311639j
0.508819875229-0.760660311639j	0.532604422088-0.744408396821j	0.55965511214-0.740759962393j
0.55965511214-0.740759962393j	0.560004344056-0.740718533339j	0.586211883749-0.738994816632j
0.586211883749-0.738994816632j	0.610711988853-0.729087191698j	0.630141989737-0.716234250184j
0.630141989737-0.716234250184j	0.630141989737-0.716234250184j	0.647925842589-0.702217002298j
0.647925842589-0.702217002298j	0.649207114152-0.701230607309j	0.667457201214-0.687512134872j
0.667457201214-0.687512134872j	0.667457201214-0.687512134872j	0.688146640479-0.675742363288j
0.688146640479-0.675742363288j	0.714345282967-0.668564298699j	0.740979019757-0.67131909421j
0.740979019757-0.67131909421j	0.741333420196-0.671346114148j	0.768601497138-0.673715017507j
0.768601497138-0.673715017507j	0.795890610928-0.664549728917j	0.816827608242-0.649548423747j
0.816827608242-0.649548423747j	0.816827608242-0.649548423747j	0.834258386943-0.631720049678j
0.834258386943-0.631720049678j	0.835448892427-0.630408948171j	0.851461741004-0.611415538687j
0.851461741004-0.611415538687j	0.851461741004-0.611415538687j	0.868691843818-0.592378364066j
0.868691843818-0.592378364066j	0.891486674794-0.573718553455j	0.918898755059-0.56156587165j
0.918898755059-0.56156587165j	0.919258054244-0.561372704771j	0.94688059537-0.544980078486j
0.94688059537-0.544980078486j	0.963740311723-0.515006729562j	0.963740311723-0.515006729562j
0.963740311723-0.515006729562j	0.966921820688-0.485190830779j	0.966921820688-0.485190830779j
0.966921820688-0.485190830779j	0.962159366157-0.456120022774j	0.954287740727-0.431679728717j
0.954287740727-0.431679728717j	0.95428740727-0.431679728717j	0.945845389898-0.40831549032j
0.945845389898-0.40831549032j	0.945305195427-0.406628931574j	0.938580759926-0.382619247377j
0.938580759926-0.382619247377j	0.938580759926-0.382619247377j	0.936057747216-0.356986623239j
0.936057747216-0.356986623239j	0.941764931359-0.328770913154j	0.957450500318-0.30634051749j
0.957450500318-0.30634051749j	0.95765110049-0.306047107676j	0.97335369178-0.284359012773j
0.97335369178-0.284359012773j	0.98023662674-0.25808129054j	0.980388425183-0.234278824754j
0.980388425183-0.234278824754j	0.980388425183-0.234278824754j	0.977632923083-0.211614549519j
0.977632923083-0.211614549519j	0.977419315746-0.210011738301j	0.974171949412-0.187601846011j
0.974171949412-0.187601846011j	0.974171949412-0.187601846011j	0.97275597599-0.164348500893j
0.97275597599-0.164348500893j	0.976425773657-0.138176975011j	0.988036761046-0.114618721513j
0.988036761046-0.114618721513j	0.988175498391-0.114295563275j	0.998541206518-0.0890447612858j
0.998541206518-0.08904476128858j	0.996358908855-0.0603207820789j	0.985906321732-0.0372091614013j
0.985906321732-0.0372091614013j	0.985906321732-0.0372091614013j	0.971599951523-0.0180575412756j
0.971599951523-0.0180575412756j	0.95476+0j	0.937920048477+0.0180575412756j
0.937920048477+0.0180575412756j	0.923613678268+0.0372091614013j	0.923613678268+0.0372091614013j
0.923613678268+0.0372091614013j	0.913161091145+0.0603207820789j	0.910978793482+0.0890447612858j
0.910978793482+0.0890447612858j	0.921344501609+0.114295563275j	0.921483238954+0.114618721513j
0.921483238954+0.114618721513j	0.933094226343+0.138176975011j	0.93676402401+0.164348500893j
0.93676402401+0.164348500893j	0.935348050588+0.187601846011j	0.935348050588+0.187601846011j
0.935348050588+0.187601846011j	0.932100684254+0.210011738301j	0.931887076917+0.211614549519j
0.931887076917+0.211614549519j	0.929131574817+0.234278824754j	0.929131574817+0.234278824754j
0.929131574817+0.234278824754j	0.92928337326+0.25808129054j	0.93616630822+0.284359012773j
0.93616630822+0.284359012773j	0.95186889951+0.306047107676j	0.952069499682+0.30634051749j
0.952069499682+0.30634051749j	0.967755068641+0.328770913154j	0.973462252784+0.356986623239j
0.973462252784+0.356986623239j	0.970939240074+0.382619247377j	0.970939240074+0.382619247377j
0.970939240074+0.382619247377j	0.964214804573+0.406628931574j	0.963674610102+0.40831549032j
0.963674610102+0.40831549032j	0.955232259273+0.431679728717j	0.955232259273+0.431679728717j
0.955232259273+0.431679728717j	0.947360633843+0.456120022774j	0.942598179312+0.485190830779j
0.942598179312+0.485190830779j	0.945779688277+0.515006729562j	0.945792050445+0.515414475223j
0.945792050445+0.515414475223j	0.94540689021+0.547532610699j	0.927879066782+0.577120227822j
0.927879066782+0.577120227822j	0.927879066782+0.577120227822j	0.903648495482+0.5947834448j
0.903648495482+0.5947834448j	0.903648495482+0.5947834448j	0.876091209976+0.605194442194j
0.876091209976+0.605194442194j	0.850989481731+0.610597561631j	0.850989481731+0.610597561631j
0.850989481731+0.610597561631j	0.826534282324+0.614968390544j	0.82480358237+0.615343847783j
0.82480358237+0.615343847783j	0.800648368168+0.621525157911j	0.800648368168+0.621525157911j
0.800648368168+0.621525157911j	0.777188358144+0.632156476879j	0.755606428497+0.651206898373j
0.755606428497+0.651206898373j	0.744023920514+0.676006197396j	0.743870120248+0.676326627149j
0.743870120248+0.676326627149j	0.732938974747+0.700769517562j	0.713623267219+0.719869175207j
0.713623267219+0.719869175207j	0.693085626398+0.731901869408j	0.693085626398+0.731901869408j
0.693085626398+0.731901869408j	0.672080037235+0.740847672207j	0.670585158335+0.741464088435j
0.670585158335+0.741464088435j	0.649553939149+0.749856732839j	0.649553939149+0.749856732839j
0.649553939149+0.749856732839j	0.628707964842+0.760257136443j	0.607877657406+0.776521037391j
0.607877657406+0.776521037391j	0.593281105102+0.798355574182j	0.593070610531+0.798637303367j
0.593070610531+0.798637303367j	0.576385628606+0.820239670927j	0.550418784084+0.832711735316j
0.550418784084+0.832711735316j	0.525177239893+0.835215339671j	0.525177239893+0.835215339671j
0.525177239893+0.835215339671j	0.501438265236+0.832401469697j	0.47738+0.826846414517j
0.47738+0.826846414517j	0.453321734764+0.821291359337j	0.429582760107+0.818477489364j
⋮	⋮	⋮

Point A	Point B	Point C
0.429582760107+0.818477489364j	0.429582760107+0.818477489364j	0.404341215916+0.820981093718j
0.404341215916+0.820981093718j	0.378374371394+0.833453158107j	0.361689389469+0.855055525667j
0.361689389469+0.855055525667j	0.361478894898+0.855337254852j	0.346882342594+0.877171791643j
0.346882342594+0.877171791643j	0.326052035158+0.893435692591j	0.305206060851+0.903836096195j
0.305206060851+0.903836096195j	0.305206060851+0.903836096195j	0.284174841665+0.912228740599j
0.284174841665+0.912228740599j	0.282679962765+0.912845156828j	0.261674373602+0.921790959627j
0.261674373602+0.921790959627j	0.261674373602+0.921790959627j	0.241136732781+0.933823653828j
0.241136732781+0.933823653828j	0.221821025253+0.952923311472j	0.210889879752+0.977366201886j
0.210889879752+0.977366201886j	0.210736079486+0.977686631638j	0.199153571503+1.00248593066j
0.199153571503+1.00248593066j	0.177571641856+1.02153635216j	0.154111631832+1.03216767112j
0.154111631832+1.03216767112j	0.154111631832+1.03216767112j	0.12995641763+1.03834898125j
0.12995641763+1.03834898125j	0.128225717676+1.03872443849j	0.103770518269+1.0430952674j
0.103770518269+1.0430952674j	0.103770518269+1.0430952674j	0.0786687900243+1.04849838684j
0.0786687900243+1.04849838684j	0.0511115045179+1.05890938423j	0.0268809332178+1.07657260121j
0.0268809332178+1.07657260121j	0.0265339962008+1.07678717999j	-0.00147370516033+1.09251268918j
-0.00147370516033+1.09251268918j	-0.035861244941+1.09212695738j	-0.035861244941+1.09212695738j
-0.035861244941+1.09212695738j	-0.0632733252059+1.07997427558j	-0.0632733252059+1.07997427558j
-0.0632733252059+1.07997427558j	-0.0860681561816+1.06131446497j	-0.103298258996+1.04227729035j
-0.103298258996+1.04227729035j	-0.103298258996+1.04227729035j	-0.119311107573+1.02328388086j
-0.119311107573+1.02328388086j	-0.120501613057+1.02197277936j	-0.137932391758+1.00414440529j
-0.137932391758+1.00414440529j	-0.137932391758+1.00414440529j	-0.158869389072+0.989143100118j
-0.158869389072+0.989143100118j	-0.186158502862+0.979977811528j	-0.213426579804+0.982346714886j
-0.213426579804+0.982346714886j	-0.213780980243+0.982373734825j	-0.240414717033+0.985128530336j
-0.240414717033+0.985128530336j	-0.266613359521+0.977950465747j	-0.287302798786+0.966180694162j
-0.287302798786+0.966180694162j	-0.287302798786+0.966180694162j	-0.305552885848+0.952462221725j
-0.305552885848+0.952462221725j	-0.306834157411+0.951475826736j	-0.324618010263+0.937458578851j
-0.324618010263+0.937458578851j	-0.324618010263+0.937458578851j	-0.344048011147+0.924605637337j
-0.344048011147+0.924605637337j	-0.368548116251+0.914698012402j	-0.394755655944+0.912974295695j
-0.394755655944+0.912974295695j	-0.39510488786+0.912932866642j	-0.422155577912+0.909284432213j
-0.422155577912+0.909284432213j	-0.445940124771+0.893032517395j	-0.460729081839+0.872424501072j
-0.460729081839+0.872424501072j	-0.460729081839+0.872424501072j	-0.470161686287+0.850459010973j
-0.470161686287+0.850459010973j	-0.47738+0.826846414517j	-0.484598313713+0.803233818062j
-0.484598313713+0.803233818062j	-0.494030918161+0.781268327962j	-0.494030918161+0.781268327962j
-0.494030918161+0.781268327962j	-0.508819875229+0.760660311639j	-0.532604422088+0.744408396821j
-0.532604422088+0.744408396821j	-0.5965511214+0.740759962393j	-0.560004344056+0.740718533339j
-0.560004344056+0.740718533339j	-0.586211883749+0.738994816632j	-0.610711988853+0.729087191698j
-0.610711988853+0.729087191698j	-0.630141989737+0.716234250184j	-0.630141989737+0.716234250184j
-0.630141989737+0.716234250184j	-0.647925842589+0.702217002298j	-0.649207114152+0.701230607309j
-0.649207114152+0.701230607309j	-0.667457201214+0.687512134872j	-0.667457201214+0.687512134872j
-0.667457201214+0.687512134872j	-0.688146640479+0.675742363288j	-0.714345282967+0.668564298699j
-0.714345282967+0.668564298699j	-0.740979019757+0.67131909421j	-0.741333420196+0.671346114148j
-0.741333420196+0.671346114148j	-0.768601497138+0.673715017507j	-0.795890610928+0.664549728917j
-0.795890610928+0.664549728917j	-0.816827608242+0.649548423747j	-0.816827608242+0.649548423747j
-0.816827608242+0.649548423747j	-0.834258386943+0.631720049678j	-0.835448892427+0.630408948171j
-0.835448892427+0.630408948171j	-0.851461741004+0.611415538687j	-0.851461741004+0.611415538687j
-0.851461741004+0.611415538687j	-0.868691843818+0.592378364066j	-0.891486674794+0.573718553455j
-0.891486674794+0.573718553455j	-0.918898755059+0.56156587165j	-0.919258054244+0.561372704771j
-0.919258054244+0.561372704771j	-0.94688059537+0.544980078486j	-0.963740311723+0.515006729562j
-0.963740311723+0.515006729562j	-0.963740311723+0.515006729562j	-0.966921820688+0.485190830779j
-0.966921820688+0.485190830779j	-0.966921820688+0.485190830779j	-0.962159366157+0.456120022774j
-0.962159366157+0.456120022774j	-0.954287740727+0.431679728717j	-0.954287740727+0.431679728717j
-0.954287740727+0.431679728717j	-0.945845389898+0.40831549032j	-0.945305195427+0.406628931574j
-0.945305195427+0.406628931574j	-0.938580759926+0.382619247377j	-0.938580759926+0.382619247377j
-0.938580759926+0.382619247377j	-0.936057747216+0.356986623239j	-0.941764931359+0.328770913154j
-0.941764931359+0.328770913154j	-0.957450500318+0.30634051749j	-0.95765110049+0.306047107676j
-0.95765110049+0.306047107676j	-0.97335369178+0.284359012773j	-0.98023662674+0.25808129054j
-0.98023662674+0.25808129054j	-0.980388425183+0.234278824754j	-0.980388425183+0.234278824754j
-0.980388425183+0.234278824754j	-0.977632923083+0.211614549519j	-0.977419315746+0.210011738301j
-0.977419315746+0.210011738301j	-0.974171949412+0.187601846011j	-0.974171949412+0.187601846011j
-0.974171949412+0.187601846011j	-0.97275597599+0.164348500893j	-0.976425773657+0.138176975011j
-0.976425773657+0.138176975011j	-0.988036761046+0.114618721513j	-0.988175498391+0.114295563275j
-0.988175498391+0.114295563275j	-0.998541206518+0.0890447612858j	-0.996358908855+0.0603207820789j
-0.996358908855+0.0603207820789j	-0.985906321732+0.0372091614013j	-0.985906321732+0.0372091614013j
-0.985906321732+0.0372091614013j	-0.971599951523+0.0180575412756j	+-0.95476+0j

Table B.2: a= 1.90952, θ= 35.66